Spatial Time-series Analysis of Satellite Derived Snow Water Equivalence
By
Carson John Quentry Farmer
B.Sc., University of Victoria, 2006

A Thesis Submitted in Partial Fulfillment of the
Requirements for the Degree of

MASTER OF SCIENCE

in the Department of Geography

Spatial Time-series Analysis of Satellite Derived Snow Water Equivalence
By
Carson John Quentry Farmer
B.Sc., University of Victoria, 2006

Supervisory committee:

_____

Dr. Trisalyn A. Nelson, Supervisor
(Department of Geography)

_____

Dr. Michael A. Wulder, Outside Member
(Pacific Forestry Centre, Canadian Forest Service)

ABSTRACT

_____

Dr. Trisalyn A. Nelson, Supervisor
(Department of Geography)

_____

Dr. Michael A. Wulder, Outside Member
(Pacific Forestry Centre, Canadian Forest Service)

_____

Dr. Gail Kucera, External Examiner
(Swiftsure Spatial Systems Inc.)

Snow cover and SWE are useful indicators of climate change. As the need to understand climate induced changes increases, so too does the need to understand the long-term spatial-temporal characteristics of snow over and SWE. In this research, we combine methods from spatial statistics, geographic information systems (GIS), time-series analysis, ecosystems classification, cluster analysis, and remote-sensing, to provide a unique perspective on the spatial-temporal interactions of snow over and SWE. We show that within the Canadian Prairies, extreme SWE are becoming more spatially constrained, and may cause some regions to be more prone to flooding. As well, we find that the temporal characteristics of SWE are not captured by current ecological management highlighting the need for Canadian ecological management units that consider winter conditions. We then address this need by developing methods designed to generate geographically distinct SWE regimes. These regimes are then used to partition the landscape into theoretical winter-based management units, and compared with conventional summer based units. We find that regional variations in the ability of

ecological units to capture SWE characteristics exist, and suggest that SWE regimes

generated as a result of this analysis should be used as guidelines for developing winter-

based management units in conjunction with current ecological classifications.

TABLE OF CONTENTS

LIST OF TABLES

LIST OF FIGURES

ACKNOWLEDGEMENTS

1.0 INTRODUCTION

1.1.   Research context

The magnitude of change and variability in climate conditions is increasing at both global and local scales. These effects are especially prevalent in polar, and other snow-covered regions (Raisanen 2001; Johannessen et al. 2004; Quayle et al. 2002; Walther et al. 2002; Robinson et al. 1993), where the increased surface albedo, sensitivity of terrestrial snow cover to atmospheric conditions and overlying air temperatures, as well as the high degree of annual and inter-annual variability (Derksen and LeDrew 2000), make regions with snow and ice susceptible to smaller changes in temperature and climate (Derksen et al. 2000). Several modeling efforts presented by the Intergovernmental Panel on Climate Change (Houghton et al. 2001) have indicated that warming in northern high-latitude regions will be approximately 40% greater than the global mean (Johannessen et al. 2004).

Significant changes in snow depth and extent has implications for local snow-melt release (Luce et al. 1998), global and regional atmospheric circulation (Gong et al. 2003; Barnett et al. 1989; Derksen et al. 1998a), as well as global and local climate and hydrological cycles (Cohen and Entekhabi 2001; Derksen and McKay 2006; Derksen et al. 2000; Wulder et al. 2007; Serreze et al. 2000). In many of these regions, snow has a significant influence on both morphological (e.g. Thorn 1978) and biological systems, such as species habitat (e.g. Karl et al. 1993), and reproductive rates (e.g. Van Vuren 1991). As well, the timing and spatial distribution of seasonal activities in both plants and animals (phenology) is often controlled by snow and climate (Walker et al. 1999; Kudo 1991;

Walther et al. 2002; McCarty 2001).

Snow is typically measured as snow water equivalence (SWE), which describes the amount of water stored within the snow-pack. SWE is an important part of global and local water budgets, as it makes up the bulk of the frozen storage term (Derksen et al. 1998). For these reasons, snow cover and SWE have been cited as useful indicators of climate change (Serreze et al. 2000; Barry 1985; Schlesinger 1986; Robinson 1993; Chang et al. 1990; Derksen et al. 2000; Goodison and Walker 1993), making the characterization of winter conditions through the analysis of SWE spatial-temporal patterns important for future climate change research.

Due to the declining costs and increasing demand for environmental monitoring at both local and global scales, the availability of large area, long-term, spatial datasets has increased. This has largely been the result of the greater use of satellite remote sensing to monitor terrestrial and marine environments. The repetitive and continuous nature of remotely sensed data presents new opportunities to examine the spatial and temporal patterns of snow and SWE over long time intervals, which is desired when attempting to isolate significant temporal trends in snow cover and SWE across the landscape (Derksen et al. 2000; Meir 2006). For example, high quality SWE datasets over large areas throughout Canada (Derksen et al. 2000; Derksen and McKay 2006; Walker and Goodison 2000) and the world (Tait 1996; Pulliainen and Halliskainen 2001) have been developed using passive microwave radiometry. The Scanning Multichannel Microwave Radiometer (SMMR 1978-1987), and the Special Sensor Microwave/Imager (SSM/I,

1987-present) provide over two decades of continuous satellite data for North America from which SWE can be derived. The large spatial and temporal extents of this dataset provide a means of examining the persistence and/or variability of observed SWE spatial patterns, outlining areas where snow cover and SWE may be more or less sensitive to climate variability.

Amalgamating ecological information at an ecosystem level provides a means to study and understand interactions between the landscape, atmosphere, and cryosphere. Furthermore, characterization of these ecosystems into ecological management units aides in organizing knowledge and generalizing complex interrelationships, highlighting geographic regions with similar ecological properties (Hirsch 1978). The analysis of pressures induced by a changing climate is facilitated by considering regions with comparable ecological properties, as these will tend to respond similarly. However, conventional large-area ecological management units (EMUs) are based largely on spring and summer landscape conditions (e.g., Rowe and Sheard 1981, Wiken 1986, Wiken et al. 1996; Ironside 1991). Indeed, the characterization of land-cover at both regional (e.g., Moody and Johnson, 2001) and global scales (e.g. Moulin et al 1997; DeFries et al, 1995, Justice et al, 1985), is frequently based on the timing of Spring green-up and Fall senescence. Using spring and summer based conditions presents a problem for understanding seasonal, or year-long climatic processes, as well as winter-based processes in regions where a substantial portion of the year is spent covered or influenced by snow. In order to effectively use snow cover and SWE to characterize winter conditions, a long-term, spatial-temporal perspective on the year-long interactions of

snow and SWE is needed. This in turn will help us understand the dynamics of cryospheric interactions with the landscape and atmosphere at various temporal and spatial scales.

1.2.   Thesis themes and objectives

This research is ultimately concerned with understanding the processes affecting snow cover by characterizing regional variations in both spatial and temporal patterns of SWE. In order to better understand the spatial-temporal patterns of snow cover and SWE, we combine two underlying themes, each with unique goals and methods. The first theme aims to quantify if and how the spatial patterns of SWE vary across the landscape, and examines how these spatial patterns vary though time. We find that within the Canadian Prairies, extreme SWE are becoming more spatially constrained though time, and may cause some regions to be more prone to flooding. In addition, significant associations between SWE spatial-temporal patterns and elevation are found, suggesting that the level of SWE variability in a particular region may be significantly impacted by the distribution of elevations in that region. These findings are considered within the context of current ecological management units, which are largely based on spring and summer landscape conditions, highlighting the need for Canadian ecological management units that consider winter conditions. The second theme examines the long-term temporal characteristics of SWE, identifying if and how they vary spatially. These results are then used to identify the spatial and temporal patterns in SWE, delineating geographically distinct SWE regimes which can be used to partition the landscape into winter based management units, or cryological management zones. Results indicate that while SWE

processes tend to operate at relatively large spatial scales, fine-scale variations in SWE temporal characteristics do exist, and may influence the overall spatial distribution of SWE across the landscape. In addition, regional variations in SWE temporal patterns are significant, and often do not correspond with current ecological management units. We highlight some of these differences, and suggest that integration of SWE regimes into current ecosystem classification systems might help to improve our understanding of climate induced changes on the landscape.

The goal of this thesis is to aide in understanding the processes affecting snow cover and SWE through long-term analysis of SWE spatial and temporal patterns. We aim to address this goal by accomplishing the following underlying objectives:

1. Chapter two examines the relationships between the spatial association of SWE and land-cover and elevation,

2. Chapter three compliments these findings by developing methods to objectively determine regional snow regimes based on the spatial and temporal patterns and trends in SWE.

3. Finally, chapter four further discusses the findings presented in this thesis, summarizing the results, and discussing the contributions, implications, and future directions of the current research.

2.0 RELATIONSHIPS WITH LAND-COVER AND ELEVATION

2.1. Abstract

Snow cover is often measured as snow water equivalence (SWE), which refers to the amount of water stored in a snow-pack that would be available upon melting. SWE is a major driver of local snowmelt release, and regional and global atmospheric circulation, climate, and hydrological cycles. Monitoring of SWE using satellite-based passive microwave radiometry has provided over two decades of continuous data for North America.

The availability of spatially and temporally extensive SWE data enables a better understanding of the nature of space-time trends in snow cover, changes in these trends, and linking these trends to underlying landscape and terrain characteristics. To address these interests, we quantify the spatial pattern of SWE by applying a local measure of spatial autocorrelation to twenty five years of mean February SWE passive microwave retrievals. Using a novel method for characterizing the temporal trends in the spatial pattern of SWE, temporal trends and variability in spatial autocorrelation are quantified. Results indicate that within the Canadian Prairies, extreme SWE are becoming more spatially constrained, and may cause some regions to be more prone to flooding. As well, results highlight the need for Canadian ecological management units that consider winter conditions.

2.2. Introduction

The spatial and temporal distributions of terrestrial snow cover impacts local snowmelt

release (Luce et al. 1998), global and regional atmospheric circulation (Barnett et al. 1989; Derksen et al. 1998a), as well as global and local climate and hydrological cycles (Derksen and McKay 2006; Derksen et al. 2000; Wulder et al. 2007; Serrezez et al. 2000). The sensitivity of terrestrial snow cover to atmospheric conditions and overlying air temperatures also makes it a useful indicator of climate change (Derksen et al. 2000; Goodison and Walker 1993). As such, examining the spatial distribution of terrestrial snow cover over time aides in understanding current and future trends in changing climate conditions (Wulder et al. 2007).

Snow cover is often measured as snow water equivalence (SWE), which refers to the amount of water (expressed as a depth in millimeters) stored in a snow-pack that would be available upon melting (NSIDC 2007). Due to issues with in situ data collection, traditional methods for snow cover and depth measurement have been spatially and temporally sparse (Walker and Goodison 2000; Wulder et al. 2007; Tait 2005). However, as climate and hydrological models have become more accurate, high quality SWE datasets over large areas throughout Canada (Derksen et al. 2000; Derksen and McKay 2006; Walker and Goodison 2000) and the world (Tait 1996; Pulliainen and Halliskainen 2001) have been developed using passive microwave radiometry.

In Canada, much of the total annual precipitation falls in the form of snow, causing snow-pack melt to be a significant portion of the total water available for stream-flow, agriculture, reservoir management, and natural processes (Brown et al. 2000; Derksen and McKay 2006; Tait 1996). This has lead the Climate Research Branch of the

Meteorological Service of Canada (MSC) to establish an ongoing program to develop algorithms for estimating SWE in open environments, as well as, coniferous, deciduous, and sparse classes of forest cover (Walker and Goodison 2000; Goita et al. 2003). Among other projects, these algorithms have been used to generate weekly SWE maps for water resource management and weather forecasting (Goodison et al. 1990; Pietroniro and Leconte 2005).

The Scanning Multichannel Microwave Radiometer (SMMR 1978-1987), and the Special Sensor Microwave/Imager (SSM/I, 1987-present) provide over two decades of continuous satellite data for North America from which SWE can be derived. The large spatial and temporal extents of this dataset provide a unique opportunity to study spatial and temporal patterns in SWE, and generate hypotheses about the spatial variability in processes influencing SWE. Consideration of large spatial and temporal extents, with relatively fine spatial and temporal resolutions, is a development over previous space-time SWE research which has emphasized spatial trends of snow cover and SWE over short time periods (e.g., Derksen et al. 1998a,1998b), or coarse-scale spatial trends (i.e. regional analysis) of snow cover and SWE for longer time-series (e.g., Brown 2000; Laternser and Schneebeli 2003).

The availability of temporally extensive geographical data on SWE enables new questions of the spatial-temporal trends in SWE to be investigated. For instance, it is possible to apply measures of spatial autocorrelation to quantify if and how SWE values deviate from a random geographical distribution (Boots 2002). In the present study,

measures of spatial autocorrelation are used to identify clusters of extreme high and low SWE values and to investigate trends over multiple years. This type of analysis can be used to locate areas of SWE abundance or absence relative to average conditions within the study region. By characterizing temporal trends in SWE clusters over multiple time periods, it is possible to examine persistence and/or variability of these spatial patterns through time, outlining areas where SWE processes may be more or less sensitive to climate variability. Furthermore, by comparing the spatial-temporal patterns in SWE with environmental data, such as land-cover, ecological systems, and elevation, hypotheses on the nature of SWE processes can be formulated.

The goal of the present paper is to quantify how the spatial patterns of SWE vary across the study region, and how these spatial patterns vary through time. The objectives are three-fold:

1. to quantify the level of spatial association and identify trends in locations of significant clusters of high or low SWE for each year in the time-series,

2. to characterize the relationship between existing ecological management units and spatial-temporal trends in SWE, and

3. to quantify how spatial-temporal trends in SWE relate to elevation.

A measure of spatial association is used to describe geographical variation in the dominant spatial patterns of SWE. Prevailing temporal trends in SWE spatial association are then quantified using a novel method for quantifying temporal trend over multiple

time periods. Locations with space-time trends that indicate the potential for sensitivity to climate variability are highlighted and the underlying landscape and terrain characteristics are related to trends in the space-time patterns of SWE.

2.3. Study area and data

2.3.1. Study area

The study region is constrained to the interior regions of the Canadian prairies, and is comprised of both the Prairies and Boreal Plains ecozones (Figure 2.1). The region was selected in part due to strong inter-annual variability in raw SWE (Wulder et al. 2007). These ecozones are defined based on the Canadian terrestrial ecozones, which are boundaries delimiting relatively homogeneous ecosystems within Canada. According to Wiken et al. (1996), an ecosystem can be defined as a unit of nature which is characterized by living and non-living elements and their interrelationships. Prairie and open tundra regions occur in the Prairie and Boreal Plains ecozones and are characterized by relatively flat, rolling plains and low-lying valleys. Vegetation is primarily restricted to shrubs and sparse treed areas, with cold winters and short warm summers. In the Prairie ecozone, approximately 25 percent of the total precipitation falls as snow (Wiken et al. 1996), providing a relatively large portion of the total annual precipitation as measurable SWE. Furthermore, according to Wulder et al. (2007), regions which may be classified as either open prairie or open tundra appear to contain the most temporally variable raw SWE estimates. As such, these areas are particularly susceptible to the impacts of climate change.
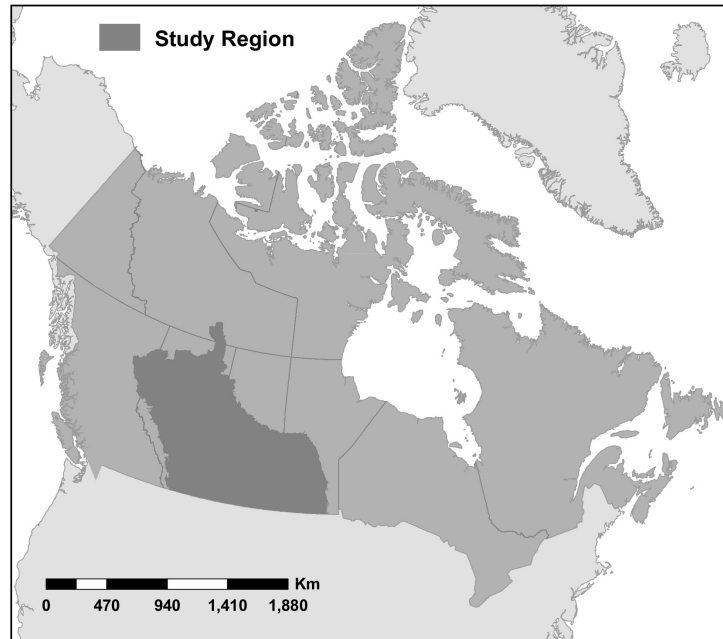
Figure 2.1: Study region includes both the Boreal Plains and Prairies Terrestrial Ecozones of central Canada.

2.3.2. Brightness temperature data

The primary data-source used for the present analysis is brightness temperatures (in Kelvin) acquired by both the SSM/I passive microwave radiometer on-board the Defense Meteorological Satellite Program (DMSP) F13 satellite and the SMMR passive microwave radiometer on-board the NIMBUS-7 satellite, which can be used to estimate SWE. The estimation of SWE from dry snow is primarily a function of changes in the scattering of naturally emitted microwave radiation caused by snow crystals, such that as the depth and density of the snow increases, the amount of volume scattering also increases (Foster et al. 1999). Given this relationship, detected microwave brightness temperature decreases with increasing snow depth due to the greater amount of snow

crystals available for volume scattering of the microwave signal (Derksen et al. 2000). Shorter wavelength energy (37 GHz) is more readily scattered by crystals in the snow-pack than the longer wavelength energy (19 GHz). Thus, to quantify SWE in millimeters, the difference between the shorter wavelength microwave energy and the longer wavelength energy can be used. Although the estimation of SWE from passive microwave brightness temperatures is theoretically simple, operational issues arise in practice. Potential complications may develop from a range of physical parameters including: snow wetness, snow crystal size, depth hoar, and ice crusts, as well as the underlying land cover, topography, and overlying vegetation (Derksen et al. 2000).

The SSM/I and SMMR data are provided in the Equal Area Scalable Earth Grid (EASE-Grid) format (see Armstrong and Brodzik 1995) from the National Snow and Ice Data Center (Knowles et al. 1999; Armstrong et al. 1994). Values represent the difference between the 37 GHz and 19 GHz vertically polarized channels, which are the conventional frequencies used to estimate SWE in most algorithms (Goodison 1989). As such, this brightness temperature difference can be used as a proxy for SWE estimates. The advantage to working with the brightness temperatures rather than actual SWE estimates is that the data are not constrained by algorithm issues, and can reduce errors induced through excess data manipulation and estimation. For the present study, February brightness temperature gradients were derived for the study area over twenty-six years (1979-2004, excluding 1994). Using mean February brightness temperature gradients allows spatial and temporal variability in spatial association to be measured when snow extent for North America is expected to be at a maximum (McCabe and

Legates 1995, Derksen et al. 2003).

2.3.3. Ecoregions and ecoprovinces

In order to provide a finer-scale spatial context with which to consider how the spatial-temporal pattern of SWE are impacted by terrestrial characteristics, the study area can be further broken down into terrestrial ecoprovinces and ecoregions. Ecoprovinces are largely based on characterizing major assemblages of structural or surface forms and faunal realms, as well as vegetation, hydrology, soil, and macro climates (Marshall et al. 1998). Ecoprovinces were created as part of an ecological framework to address the environmental concerns of the Commission for Environmental Cooperation (CEC) by Canada, Mexico and the United States (Marshall and Schut 1999). Subsequently, ecoregions subdivide the terrestrial ecoprovinces, and are characterized by distinctive large order landforms or assemblages of regional landforms, small order macro- or meso-climates, vegetation, soil, and water features (Wiken et al. 1996). These ecological units are useful for describing the major driving factors of an ecosystem, and as such are useful for conservation planning and analysis (Kerr and Deguise 2004). The six terrestrial ecoprovinces, and twenty-nine ecoregions in the study area are presented in Table 1, in addition, Figure 2.2 shows the boundaries of the individual ecoregions.

2.3.4. Elevation

Spatial-temporal patterns in SWE are also interpreted using elevation, enabling an assessment of the relationship between SWE spatial-temporal features and ground-surface characteristics. Elevation data are obtained from a digital elevation model

(DEM) with a 1 km spatial resolution. The DEM (GTOPO30) is a global digital elevation model produced as part of a collaborative effort led by the US Geological Survey's (USGS) EROS Data Center (Gesch et al. 1999). It is reported to be accurate to within ± 30 m in most areas (Defense Mapping Agency 1986; US Geological Survey 1993). The DEM will be used to determine elevation, which may have some bearing on the amount and type of snow deposition.

Table 2.1: List of Ecoregions and associated Ecozone and Ecoprovince.

Ecozon	Ecoprovince	Ecoregion	Description
Boreal Plains	Central Boreal Plains	Slave River Lowland (136)	Subhumid mid-boreal ecoclimate, with cool summers and long, cold winters.
	Boreal Foothills	Clear Hills Upland (137)	Cool, short summers and cold winters with severe temperatures moderated by frequent
	Central Boreal Plains	Peace Lowland (138)	Subhumid, low boreal ecoclimate, marked by warmer summers than the surrounding areas.
	Central Boreal Plains	Mid-Boreal Uplands (139)	Upland area, with subhimid mid-boreal ecoclimate, short, cool summers and cold winters.
	Central Boreal Plains	Mid-Boreal Uplands (140)	Upland area, with subhimid mid-boreal ecoclimate, short, cool summers and cold winters.
	Central Boreal Plains	Mid-Boreal Uplands (141)	Upland area, with subhimid mid-boreal ecoclimate, short, cool summers and cold winters.
	Central Boreal Plains	Wabasca Lowland (142)	Lowland area, with subhumid mid-boreal ecoclimate, and cool summers and long, cold
	Central Boreal Plains	Western Boreal (143)	Poorly drained, low-relief plain, with cool, short summers and cold winters.
	Central Boreal Plains	Mid-Boreal Uplands (144)	Upland area, with subhimid mid-boreal ecoclimate, short, cool summers and cold winters.
	Boreal Foothills	Western Alberta Upland (145)	Upland area, marking transition between mid-boreal and mid-cordilleran vegatation.
	Boreal Foothills	Western Alberta Upland (146)	Upland area, marking transition between mid-boreal and mid-cordilleran vegatation.
	Central Boreal Plains	Mid-Boreal Uplands (147)	Upland area, with subhimid mid-boreal ecoclimate, short, cool summers and cold winters.
	Eastern Boreal Plains	Mid-Boreal Lowland (148)	Upland area, with subhimid mid-boreal ecoclimate, short, cool summers and cold winters.
	Central Boreal Plains	Boreal Transition (149)	Transition zone, with subhumid low boreal ecolimate, and warm summers and cold winters.
	Central Boreal Plains	Mid-Boreal Uplands (150)	Upland area, with subhimid mid-boreal ecoclimate, short, cool summers and cold winters.
	Central Boreal Plains	Mid-Boreal Uplands (151)	Upland area, with subhimid mid-boreal ecoclimate, short, cool summers and cold winters.
	Central Boreal Plains	Mid-Boreal Uplands (152)	Upland area, with subhimid mid-boreal ecoclimate, short, cool summers and cold winters.
	Central Boreal Plains	Mid-Boreal Uplands (153)	Upland area, with subhimid mid-boreal ecoclimate, short, cool summers and cold winters.
	Central Boreal Plains	Mid-Boreal Uplands (154)	Upland area, with subhimid mid-boreal ecoclimate, short, cool summers and cold winters.
	Eastern Boreal Plains	Interlake Plain (155)	Subhumid low boreal ecoclimate, with warm summers and cold winters.
Prairies	Parkland Prairies	Aspen Parkland (156)	Transitional grassland ecoclimate, with short, warm summers, and long, cold winters.
	Central Grassland	Moist Mixed Grassland (157)	Northern extension of open grasslands in Interior Plains, with semiarid moisture conditions.
	Central Grassland	Fescue Grassland (158)	Part of Rocky Mountain foothills, with warm summers and mild winters controlled by
	Central Grassland	Mixed Grassland (159)	Semiarid grasslands region, with summer moisture deficits, and low annual precipitation.
	Central Grassland	Cypress Upland (160)	Upland region, with cooler, more moist climate than surrounding ecoregions.
	Parkland Prairies	Aspen Parkland (161)	Transitional grassland ecoclimate, with cold winters with continuous snow cover.
	Eastern Prairies	Lake Manitoba Plain (162)	Transitional zone, with warmest and most humid regions in the Canadian prairies
	Parkland Prairies	Boreal Transition (163)	Elevated upland area, with high annual precipitation.
	Parkland Prairies	Boreal Transition (164)	Elevated upland area, with high annual precipitation.

2.4.   Methods

2.4.1.   Quantifying spatial patterns

Quantifying the spatial interaction of localized areas within a study region provides

information on the location, type, and magnitude of local SWE extremes. Aspatial

analysis generalizes spatial trends, but by implicitly considering the spatial distribution of

SWE within a study region, new patterns and variability emerge, and can be quantified.

The Getis and Ord Gi* statistic (Getis and Ord 1992; Ord and Getis 1995), is a local

measure of spatial association designed to highlight spatial clusters of similarly high or

low values that are extreme relative to average trends in the data (Boots 2002). The Gi*

statistic assigns a measure of the level of spatial association at each individual pixel,

highlighting areas which display strong brightness temperature gradients (both high and

low).

In general, the G_i* statistic is designed to compare spatially local averages to global

averages by considering both the locational, and attribute relationship between each pixel

(i) and its surrounding neighbours (j) (Boots 2002). Formally, the Gi* statistic is given as

$$G_i{}^* = \sum_j w_{ij} y_{ij} \Big/ \sum_j y_{ij}$$
,

where wij defines the locational relationship between i and j, and is given a value of one

if i and j are neighbours, and zero otherwise. The attribute relationship is defined by y_{ij},

In this sense, the G_i* statistic is the sum of pixel values within a neighbourhood centered

on i, relative to the sum of all pixel values within the study region (Boots 2002). Ord and

Getis (1995) derive a standardized version of the G_i^* statistic, whose values are reported

in z-score standardized form. Using z-scores, analysis using G_i^* is suitable for

comparison between different time periods and datasets. For details on this standardized

form, see Ord and Getis (1995). All reported G_i^* results in the current paper are given in

the standardized form.

In order to maintain the finest spatial grain of analysis possible while maintaining

stability of the G_i^* statistic, the locational relationship in this analysis is based on all

pixels within a 3 x 3 grid surrounding the target location i. This ensures neighbourhoods

have a minimum of 9 pixels (inclusive), which is the above the suggested minimum

neighbour size required to maintain validity of the statistic (Boots 2002; Griffin et al.

1996). Due to issues of spatial dependence and multiple testing, which are problematic

for many local spatial statistics, it is often best to consider G_i^* results as exploratory

rather than confirmatory (Boots 2002; Sokal et al. 1998a, 1998b).

When interpreting the standardized G_i^* z-score values, a high value of G_i^* (strong

positive) indicates clustering of extreme high values, and a low value of G_i^* (strong

negative) indicates clustering of extreme low values. Mid-range values of G_i^* can be

caused by both clustering of values that are near the average global value, as well as an

absence of clustering (Tiefelsdorf and Boots 1997). Therefore, the G_i^* statistic is useful

for capturing spatial clusters of values that are extreme relative to the mean.

In the current analysis, G_i^* z-score values are categorized into three classes: greater than

or equal to 2 standard deviations from the mean indicates a cluster of high values, less

than or equal to -2 standard deviations from the mean indicates a cluster of low values, and greater than -2 and less than 2 standard deviations from the mean indicates no significant clustering in extreme values. This classification scheme allows the computed statistics to be visualized, clearly highlighting areas of significant clustering with respect to the mean, and is the standard approach to interpreting G_i^*. In addition, where measures of temporal variability require discrete values (modal state), this classification provides a representation of the computed G_i^* values which is not continuous.

2.4.2.   Inter-annual spatial association

Computing the G_i^* statistic for each successive year $(y_i - y_n)$ in the study period provides a means for inter-annual comparison of the spatial pattern in extreme SWE values. To aid interpretation, a cluster of SWE is defined as a grouping of spatially adjacent significant values (both high and low). Scatterplots which examine the relationship between the number of significant pixels in the study region (significant spatial autocorrelation in both high and low SWE), and the number of significant clusters (both high and low SWE) were generated to compare how clusters of extreme SWE change relative to the overall abundance or absence of extreme values. Exploratory analysis indicated that relationships between the number of clusters and pixels differed in two time periods: 1979-1988 and 1989-2002, and by generating scatterplots for each time period we highlight how the spatial processes of SWE change through time. To compare differences in the slope of the observed relationships (number of clusters vs. pixel, comparisons between different temporal windows were performed using standard t-tests.

2.4.3. Temporal variability and trends

Changes in the level of spatial association through time were quantified to assess inter-annual trends in G_i^* results. A spatial grid of individual time series' was generated, each with its own temporal signature. These time-series' were then individually analyzed for temporal trends and variability using methods which treat each pixel within the study region as a separate temporal vector. This is a novel use of SWE time-series data, in that each time-series is analyzed within a larger spatial context. Temporal analysis is primarily concerned with decomposing a time-series into trends, variations, and other temporal characteristics (Chatfield 1975). Different measures may be employed which describe and explain the temporal characteristics of a time-series in order to make inferences about the underlying generating process.

Several measures were used to quantify temporal trends in the SWE data. The observed SWE time series' were compared to hypothetical random SWE time-series' to assess the hypothesis that the temporal SWE observations are independent and identically distributed along the time-series, and thus equally likely to have occurred in any order (Kendall and Ord 1990). To assess hypotheses of randomness in the time-series, turning points were used. Turning points may be defined as either a peak or trough within a time-series, and usually refers to a value which is either greater than (peak) or less than (trough) its neighbouring values (Kendall and Ord 1990). The test statistic (p) is a count of the number of peaks and troughs in the time-series, and according to Kendall and Ord (1990), as the total number of time periods (n) increases, the distribution of the test statistic approaches normality, with an expected value of *(2n – 4) / 3*, and variance equal

to *(16n – 29) / 90*. Thus, the statistic may be represented as a standard variate, such that:

$$z(p) = \frac{p - E(p)}{[\mathrm{var}(p)]^{1/2}} \, .$$

Two descriptive measures provide further insight into the temporal patterns of SWE

observed in the study area: relative variability, and the modal state of each individual the

temporal vector. The relative variability of SWE spatial association, which is simply the

count of the number of state changes (the number of times a value increases or decreases

from a previous value in the time-series), and the modal state of the time-series. Where

ties in the modal state occur, the modal value which occurs first in the time-series is

given.

2.4.4.   Comparison with ecoregions and elevation

Comparing the distribution of temporal metrics between ecoregions, as well as comparing

the distribution of elevations for different temporal metrics, provides insight into the

characteristics of these different spatial and temporal features. Ecoregions were

intersected with images of variability in SWE spatial autocorrelation for each pixel in the

study region. A quantitative comparison of the distribution of pixels with statistically

significant variability (both high and low) in $G_i{}^*$ z-scores over each ecoregion was

performed using a Mann-Whitney U test (Hollander and Wolfe 1999; Mann and Whitney

1947). This highlights ecoregions which display significantly different distributions of

variability in computed $G_i{}^*$ z-scores, highlighting the differences in variability between

ecoregions, as well as outlining areas where the spatial-temporal pattern in SWE

variability is not captured by the current ecological management units defined by the ecoregions.

Relationships between the temporal trends in SWE spatial autocorrelation and elevation were quantified using the Mann-Whitney U test to compare variations in elevation for both variability and modal state classes. By classifying modal states into two different classes: spatial autocorrelation of high SWE (high), and spatial autocorrelation of low SWE (low), the frequency distributions of elevations for each modal state class were quantified. A similar comparison was performed for variability classes, in which variability was classified into significantly high variability in G_i^* z-scores, and significantly low variability in G_i^* z-scores, to again compare elevation frequency distributions.

2.5.   Results

2.5.1.   Inter-annual spatial association

The spatial distribution of clustering in extreme SWE values is variable over the study region and through time. The relationship between individual significant pixels and significant clusters gives an indication of the pattern of spatial association within the study region in any given year. Initial analysis revealed a break in the observed relationship between 1988 and 1989. Figure 2.3a shows the relationship between the number of individual significant pixels (spatial autocorrelation in both high and low SWE), and the number of significant clusters of SWE values (spatial autocorrelation in both high and low SWE) from 1979-1988. As the number of individual significant pixels

increases, the number of contiguous clusters also increases, indicating that pixels with

positive spatial autocorrelation in extreme high SWE values are occurring as smaller

isolated pockets, rather than contributing to existing clusters. The observed relationship

for significant spatial autocorrelation of pixels and clusters of high SWE is significant at

alpha = 0.05 (t = 7.016, p-value = 0.000); whereas, significant spatial autocorrelation in

low SWE is not significant (t = 0.314, p-value = 0.762).
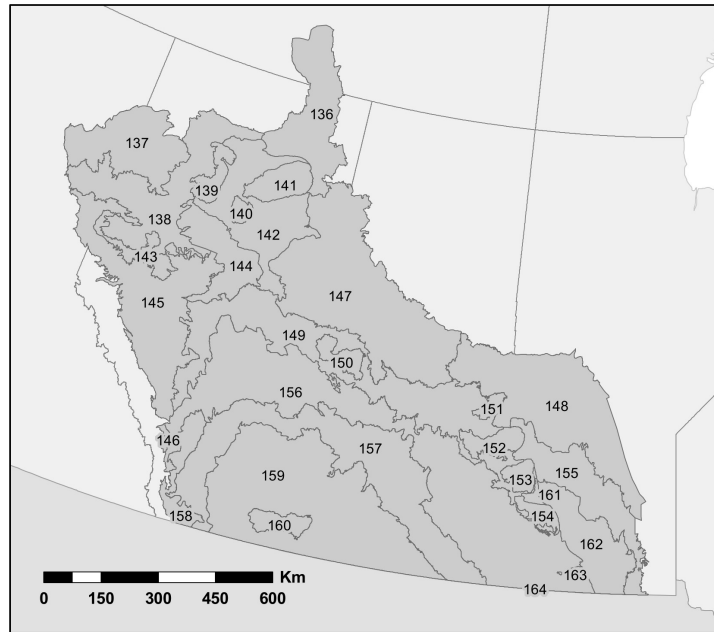
Figure 2.2: Terrestrial ecoregion boundaries across the study region. Each number is the unique identifier for the corresponding ecoreigon, these values are given in Table 1.

Figure 2.3b presents the number of individual significant pixels (spatial autocorrelation in

both high and low SWE) with respect to the number of significant clusters (spatial

autocorrelation in both high and low SWE) for the years 1989-2004. The relationship

between the number of individual significant pixels (spatial autocorrelation in both high

and low SWE) and the number of individual clusters (spatial autocorrelation in both high and low SWE) is roughly inverse in both cases, such that, in general, as the number of significant pixels (or total area that the clusters occupy) increases, the number of clusters decreases. This indicates that the scale of spatial association in extreme SWE processes is increasing through time, and that significant pixels are contributing to large, spatially constrained clusters.

While the relationships between individual significant pixels and significant clusters of spatial autocorrelation in both high and low SWE within the 1989-2004 time period are not significant, the difference in the slope of the relationship between the two time periods (a and b) for significant spatial autocorrelation in high SWE is significant ($t =$ 22.609, p-value = 0.000). This is further evidence that prior to 1989, SWE spatial processes were different, with extreme events less spatially constrained than during the 1989-2004 time period.

2.5.2. Relationships with ecoregions and elevation

Characterization of the relationship between existing ecological management units and the spatial-temporal trends in SWE, was given by an initial evaluation of relative variability for each ecoregion using the Mann-Whitney U test. When comparing the distribution of relative variability values within each ecoregion with the distribution of relative variability values of all other ecoregions, in most cases no significant differences were observed (p-values >0.05). Only a single ecoregion in the periphery of the north-western portion of the study region was found to display a significantly different

distribution of relative variability values (Z-value = -6.71, p-value = 0.000). The Clear

Hills Upland, located in the Boreal Plains ecozone displayed a range in relative

variability values which was significantly smaller than the rest of the study region, and

showed no significant variability along the time-series. Figure 2.4 shows the distribution

of variability values throughout the study region. The distribution of variability values

throughout the study region has a clear spatial component, with similar levels of

variability occurring together across the landscape (Moran's I = 0.559 p-value = 0.010).

For information on the Moran statistic, see (Cliff and Ord 1981). However, the

distribution and boundaries of the ecoregions do not coincide with the distribution of

variability values (see Figure 2.2 for ecoregion boundaries).
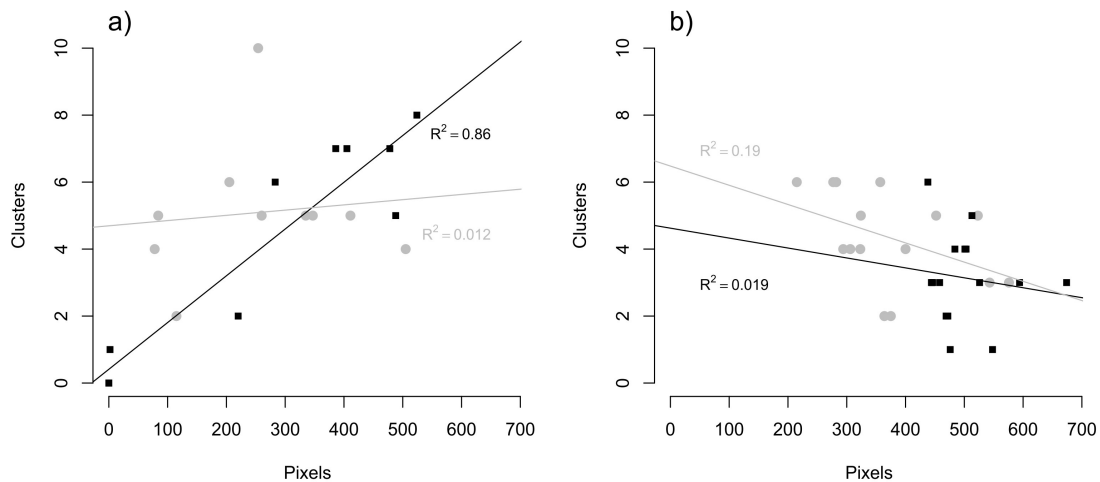
Figure 2.3: Relationship between the number of individual pixels which show statistically significant spatial autocorrelation (both high and low SWE) and the number of contiguous clusters of statistically significant pixels. Note: relationship from 1979-1988 (a) is significantly different than from 1989-2004 (b).

The distribution of elevations for modal state classes showing significant spatial

autocorrelation in both high and low SWE values were found to be significantly different

from each other, as well as from the study area as a whole (p-values <=0.05). Figure 2.5

shows the distribution and summary statistics of elevations for significant spatial

autocorrelation in high SWE values (Figure 2.5a), and low SWE values (Figure 2.5b)

respectively. While the number of pixels in the study region displaying spatial

autocorrelation in high SWE values (n = 423) is larger than the number of pixels

displaying significant spatial autocorrelation in low SWE values (n = 231), the level of

dispersion is lower for spatial autocorrelation in low SWE values (CV = 0.22 vs CV =

0.48). This is partly influenced by the bimodal shape of the distribution of elevations in

Figure 2.4b. Statistically significant spatial association in low SWE values occurs

primarily over regions where elevations are ±1 standard deviation (>860.06 m or <341.24

m) from the mean elevation (600.65 m); therefore, spatial autocorrelation of low SWE

values is restricted to the more 'extreme' elevations in the study region, particularly in the

lowland regions, where over 40 percent of the data in this class are found.
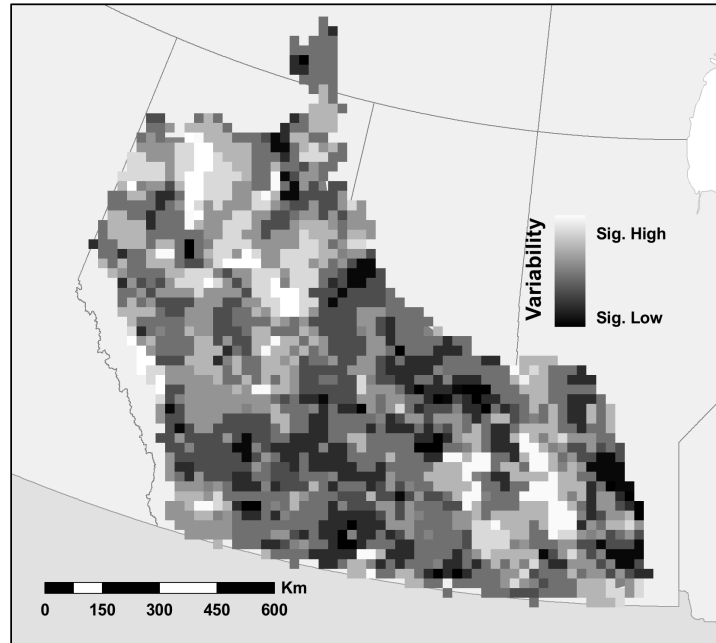
*Figure 2.4: Spatial distribution of SWE temporal variability across
the study region. Lighter values correspond to significantly high
temporal variability in SWE values, whereas darker values
correspond to significantly low temporal variability in SWE values.*

Classifying variability into two statistically significant classes: significantly high

variability in the spatial association of SWE through time (high variability), and

significantly low variability in the spatial association of SWE through time (low

variability), separates regions with significant variability in SWE spatial association from

the remainder of the study region, and allows differences in the distributions of elevations

between these two classes to be assessed. The Mann-Whitney U test indicates that the

distribution of elevations for the low variability class is significantly different from the

high variability class (Z-value = -4.13, p-value = 0.00). Figure 2.6 characterizes how

elevation is different between the high and low variability classes. Although the

distributions of elevations for both classes are negatively skewed, the range in elevations

is significantly different between the two classes (max. (high variability) = 1334.17 m vs.

max. (low variability) = 2438.14 m). As well, the elevations in Figure 2.5b fall into two

clear groupings, with the majority of values occurring close to the mean (644.76 m), and

the rest of the values, in regions with significantly high elevations (± 2 standard

deviations from the mean). The differences in the range and distribution of elevations

between these two classes are likely due to the spatial distribution of the variability

values: all pixels which are characterized by significantly high variability in SWE spatial

association are located in the northwestern and southeastern portions of the study region,

with no pixels having high variability in SWE values through the central portion of the

study region. This is contrasted by pixels which are classified as having significantly low

temporal variability in SWE values, which are located randomly throughout the study

region, and occur only in relatively small, isolated clusters of approximately 200 km2 on

average.
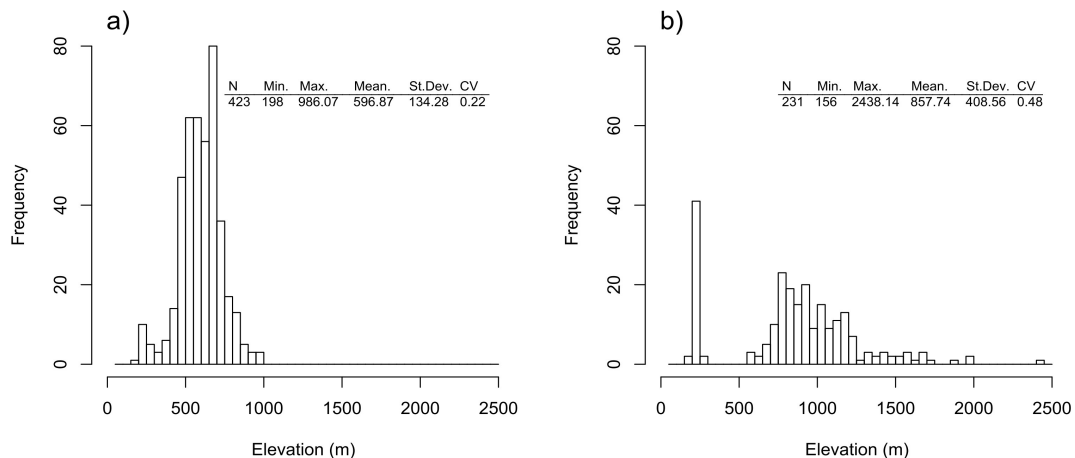
Figure 2.5: Distribution and summary of elevations for regions with statistically significant spatial autocorrelation in both high (a), and low (b) SWE. Note: CV = Coefficient of Variation (Std. Dev./Mean).
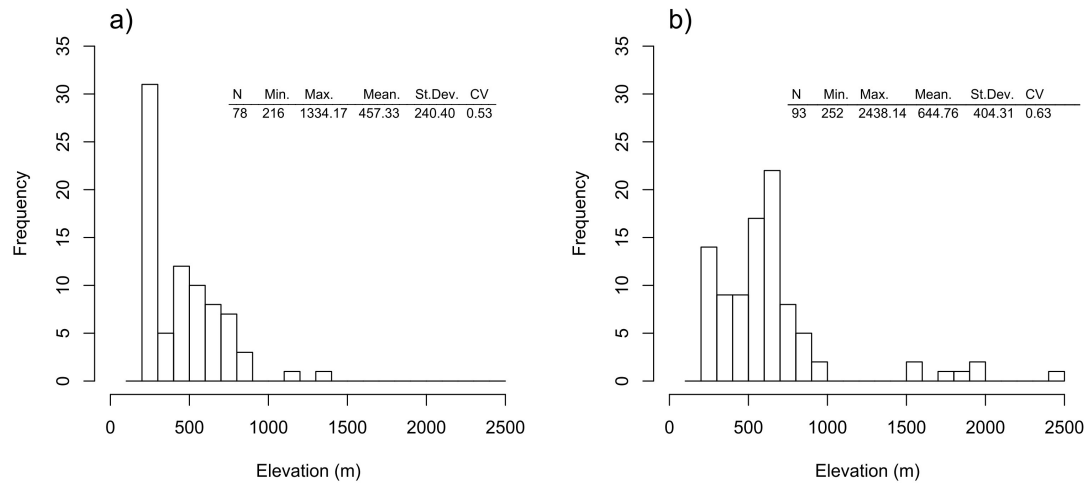
Figure 2.6: Distribution and summary of elevations for regions with significantly high variability (a), and significantly low variability (b). Note: CV = Coefficient of Variation (Std. Dev./Mean).

2.6.   Discussion

Significant spatial association occurred within the study region in most years, and the level of spatial association in SWE varies through both space and time. While the number of individual pixels showing significant spatial autocorrelation in both high and low SWE was increasing throughout the study period, they tended to coalesce into larger, contiguous regions of extreme (both high and low) SWE. These larger regions appear to coalesce towards the center of the study area, and are potentially important drivers of atmospheric processes (e.g. Dewey 1977; Namias 1985; Liu and Yanai 2002; Gong et al. 2004), as well as potentially sensitive to the effects of changing climate conditions (Bednorz 2004; Keller 2005).

The relationship between the number of individual significant pixels and contiguous clusters showing spatial autocorrelation in high SWE displayed significant variation through time. Extreme high SWE tended to become more spatially constrained after 1989, and large clusters occurred through the middle of the study region, in the northern portion of the Prairies ecozone, and Southern portion of the Boreal Plains ecozone. The region primarily comprises the Moist Mixed Grasslands, Aspen Parklands and Boreal Transition ecoregions of the Central Grassland and Parkland Prairies ecoprovinces, and to a lesser extent, the Slave River Lowland ecoregion in the northern reaches of the Boreal Plains Ecozone. In general, this group of ecoregions extends in a broad arc from southwestern Manitoba, north-westward through Saskatchewan to its northern apex in central Alberta. As the climate continues to become more variable, the potential for flooding may be significantly altered in regions supplied by these areas (Olsen et al. 1999; Barnett et al. 2005). This relationship was not observed in the spatial autocorrelation of low SWE values, where the relationship between individual significant pixels and significant clusters remains non-significant over both time periods (1979-1988 and 1989-2004), suggesting that the level and extent of clustering in dry winter conditions does not appear to be confined to any specific region.

While in some instances the Canadian terrestrial ecoregions may help to characterize some of the variability and trends in the spatial association of SWE, to a large degree these ecological units do not provide sufficient explanation for the observed spatial-temporal patterns in SWE. Differences in the variability of SWE spatial autocorrelation across the study region were observed, and displayed a significant spatial component.

These differences were generally not related to ecoregions, which highlights the need for ecological management units which take into account SWE and other dominant winter processes. Ecoregions, and many other ecological management units, are generally based on spring and summer conditions, and as a result do not properly represent snow and winter conditions. In many regions of Canada, a large portion of the year is spent with snow, and any models or management strategies that include winter processes would benefit from a new classification systems which partitions the landscape with consideration to SWE, and other winter conditions.

Several trends emerged in the relationships between space-time trends in SWE and elevation. Firstly, regions of high and low temporal variability in SWE spatial patterns display significantly different distributions of elevation, suggesting that processes relating to SWE variability may be linked with elevation and/or some associated phenomenon, for example temperature or net radiation. Classifying pixels by modal state provides further evidence for a linkage between elevation and the spatial-temporal aspects of SWE spatial association. Regions of consistent spatial autocorrelation in high SWE were shown to be significantly different in terms of elevation from regions of consistent spatial autocorrelation in low SWE. A clear spatial separation of regions of consistently high modal state from regions of consistently low modal state was observed, and elevation was shown to be a strong determinant of this relationship. Low modal states occurred only in relatively extreme elevations throughout the study region, and showed no overlap with regions of high consistent SWE spatial autocorrelation. In general, elevation has proven to be a relatively effective indicator of SWE spatial-temporal patterns across the study

region, and while elevation has often been linked to SWE processes, the current analysis shows that as climate variability continues to increase over time. Elevation may also be a useful indicator of changing trends in SWE spatial and temporal patterns, with the greatest levels of variability anticipated to occur over elevation extremes, such as upland and lowland regions.

2.7. Conclusions

Despite difficulties in characterizing SWE spatial-temporal features using current ecological management units, several dominant patterns in SWE spatial autocorrelation do emerge, and are captured by the various temporal metrics employed in the current analysis. Results revealed that the number of locations having significant spatial autocorrelation within the study region have increased both in number and size throughout the study period. These regions have continued to grow and coalesce into larger, contiguous regions of extreme SWE, particularly after 1989, where extreme high SWE has tended to become increasingly constrained to the grassland, parkland, and transition zones of the Central Grassland and Parkland Prairies ecoprovinces. This indicates that as the climate in these regions becomes more variable through time, some areas will become more prone to extreme whether conditions, leading to droughts, and/or flooding in localized regions such as the surrounding Mid-Boreal Uplands regions, and lowland planar regions to the east. This has implications for SWE runoff prediction, flood forecasting, and water resource management, which need to take into account the spatial nature of SWE. Furthermore, the relationships between the temporal characteristics of SWE and elevation have revealed that the level of SWE variability in a

particular region may be significantly impacted by the distribution of elevations in that region, providing evidence for elevation-controlled SWE processes not captured by the ecoregions. The observed relationship between SWE variability and elevation, coupled with knowledge of the changing spatial configuration of SWE clusters through time indicates that regions of variable topography, such as those located in the northwestern portion of the Central Boreal Plains ecoprovince, may be differentially impacted by changing climate conditions.

Future research will use the detected spatial-temporal patterns of SWE to distinguish unique regimes of snow cover across Canada. SWE regimes describe the regular spatial and temporal patterns of SWE accumulation in individual regions, and are a major control of spatial and temporal patterns and processes in many ecosystems (Walker et al. 1999). Knowledge of the distribution of these SWE regimes will help analysts answer key questions regarding their impact on human and ecological processes. Further, based upon these findings, new ecological units could be developed that also integrate winter snow cover characteristics with the existing suite of determinants mainly based upon summer land cover conditions.

The methods demonstrated in this article may have benefit to other research which focuses on large-area, spatial-temporal datasets collected over long time periods. By characterizing the temporal signature of spatial patterns over multiple time periods, it is possible to generate a mappable representation of the spatial-temporal data which is both intuitive and informative. Furthermore, by employing more complex temporal modeling

and trend detection techniques as part of this overall methodology, analysts in fields such as water resource management, wildlife management, climate change research, and forestry may quantitatively characterize trends through time, and develop new knowledge to support management.

3.0 DETERMINATION OF CANADIAN SNOW REGIMES

3.1. Abstract

Ecological management units organize knowledge and generalize complex interrelationships, providing a means to identify geographic regions with similar properties. In Canada, standard ecological units are based largely on spring and summer landscape conditions. This may be problematic for understanding the interactions of winter-controlled processes. The spatial and temporal patterns of SWE accumulation and melt influence many winter-based ecological systems, and are therefore useful for characterizing winter-based processes.

In this paper, we examine the long-term temporal characteristics of SWE, and identify if and how they vary across the landscape in order to delineate geographically distinct SWE regimes. These SWE regimes are then compared with current spring and summer based ecological management units. Results indicate that high variability in melt rates and seasonal activity, combined with an abundance of SWE, provide highly sensitive regions with strong SWE gradients that are not captured by conventional ecological management units. However, where SWE tends to be low, and variability minimal, regions based on spring and summer conditions provide an acceptable representation of winter processes. We suggest that the SWE regimes generated as a result of this analysis should be used as guidelines for developing winter-based management units in conjunction with current ecological classifications.

3.2. Introduction

Ecological management units organize knowledge and generalize complex interrelationships, providing a means to identify geographic regions with similar properties (Hirsch 1978). Such geographic regions tend to respond similarly to disturbances and pressures, and by defining ecological management units it is possible to generalize knowledge regarding the spatial and temporal processes affecting a region (Hirsch 1978). Ecological management units thus aid in the description, characterization, and delineation of physical processes necessary for scientific modeling, management, and conservation of ecosystems (Blasi et al. 2000; Sims et al. 1996). As well, ecological management units are essential for extrapolating research results from single locations to larger areas.

In Canada, standard ecological units are based largely on spring and summer landscape conditions (e.g., Rowe and Sheard 1981, Wiken 1986, Ironside 1991). Temporally, it is often Spring green-up and Fall senescence that are used for characterizing landcover at both regional (e.g. Moody and Johnson, 2001) and global scales (e.g. Moulin et al 1997; DeFries et al, 1995, Justice et al, 1985). This may be problematic for understanding the interactions of winter-controlled processes, such as spring snow-melt and runoff, or for regions where a substantial portion of the year is spent covered with snow. Terrestrial snow cover is a significant driver of many global and regional climatological systems, including atmospheric circulation (Barnett, Adam, and Lettenmaier 2005; Derksen et al. 1998a), and climate and hydrological cycles (Serreze et al. 2000; Derksen et al. 2000; Wulder et al. 2007). The relatively high surface albedo, and high degree of inter-annual variability in snow extent, are unique properties which inherently affect the cryosphere-

climate system (Chang et al. 2003; Derksen, Ledrew, and Goodison 2000). The current suite of ecological management units in Canada do not sufficiently consider these physical processes.

The spatial and temporal patterns of SWE accumulation and melt influence the spatial and temporal patterns and processes of many ecological systems. For example, the spatial distribution of snow impacts meso-scale processes of biological systems in arctic and alpine ecosystems (Walker et al. 1993; Walker et al. 1999). As well, spatial-temporal patterns of SWE influence biodiversity monitoring (Duro et al. 2007), species and community distributions (Walker et al. 1999), and many anthropogenic processes such as tourism, recreation, and urban and agricultural water supply (Walker et al. 1999). Analyzing regional variations in SWE spatial-temporal patterns will highlight unique SWE regimes, or groups of locations with similar spatial and temporal interactions of SWE. SWE regimes are useful for assessing the impact of snow cover and SWE on abiotic and biotic systems within a region and, like ecological units, provide a mechanism for extrapolating winter processes observed at specific locations to landscapes. The goals of this paper are to examine the long-term temporal characteristics of SWE, and identify if and how they vary across the landscape, in order to delineate geographically distinct SWE regimes. These SWE regimes can then be used to partition the landscape into winter based management zones, and compared with current Spring and Summer based ecological management units. These goals are guided by four primary objectives:

1. to apply an advanced curve fitting procedure, which takes into account features

and fall-backs of the SWE dataset, to a temporal sequence of passive microwave derived SWE estimates,

2. to derive annual and inter-annual temporal metrics relating to SWE variations through time based on the fitted curve,

3. to delineate geographically distinct winter-based management zones by clustering temporal metrics generated for local regions within the study area, and

4. to examine the variability of winter conditions derived from the SWE regimes within current spring and summer ecological management units.

The repetitive and continuous nature of remotely sensed data, provide a means of capturing both short-term and long-term spatial-temporal variations and patterns, which is desired when attempting to isolate significant temporal trends in snow cover and SWE across the landscape (Derksen et al. 2000; Meir et al. 2006). This allows the nature of intra and inter-annual fluctuations in SWE variations to be characterized, and provides important data for differentiating SWE regimes. Over the past two decades, large area SWE datasets collected throughout Canada (Derksen, Ledrew, and Goodison 2000; Derksen and MacKay 2006; A Walker and Goodison 2000) and the world (Tait 1996; Pulliainen and Hallikainen 2001; Grody and Basist 1996) have been developed using passive microwave radiometry. These datasets have largely been the result of SWE algorithm development based around the Scanning Multichannel Microwave Radiometer (SMMR), and the Special Sensor Microwave/Imager (SSM/I) (Derksen, et al. 2005), and

have been used for research on the interaction between snow cover and climate (Derksen et al. 2000), as well as validation of regional climate models (MacKay et al. 2003). We limit our analysis to the SSM/I satellite record, which provides continuous satellite data records for North American collected daily since 1988 (Derksen et al. 2005). Due to the inherent characteristics of space-borne passive microwave data, such as all-weather imaging, frequent overpass times, the ability to quantify SWE, and an existing long-term time series (Derksen et al. 2002; Derksen et al. 2005; Sokol et al. 2003; Derksen et al. 2000), these datasets are appropriate for SWE regime characterization. By taking advantage of both the fine spatial and temporal resolutions of current passive microwave derived SWE datasets, this research provides insight not accessible by conventional space-time SWE research which has emphasized spatial trends of snow cover and SWE over short time periods (e.g. Derksen et al., 1998b,1998c), or coarse-scale spatial trends (i.e. regional analysis) of snow cover and SWE over longer time periods (e.g., Brown, 2000; Laternser and Schneebeli, 2003).

3.3. Study area and data

3.3.1. Deriving SWE from passive microwave radiometry

Theoretical estimation of SWE from passive microwave radiometry is primarily a function of the interaction of snow crystals with the microwave radiation naturally emitted by the earth, and assumes that as the depth and density of snow increases, scattering of the passive microwave signal also increases (Foster et al., 1999). In general, shorter wavelength energy (37 GHz) is more readily scattered by crystals in the snow-pack than the longer wavelength energy (19 GHz), allowing the difference between these

two satellite measured frequencies to be used to estimate SWE (Foster et al, 1999; Walker and Goodison, 2000). In regions where interactions between the atmosphere, snow cover, and the underlying ground surface is complex, such as highly mountainous regions, or regions with dense forest cover, complications may arise in the estimation of SWE from passive microwave brightness temperatures (Tait, 1996; Pullianinen and Hallikainen, 2001; Foster et al., 1999). These complications derive from a range of physical parameters including: snow wetness, snow crystal size, depth hoar, and ice crusts, as well as the underlying land cover, topography, and overlying vegetation (Derksen et al., 2000).

Estimation of SWE from passive microwave radiometry is further complicated by factors relating to topography and overlying vegetation. This occurs as the microwave emission and scattering characteristics of the overlying vegetation affects the naturally emitted energy of the underlying ground surface (Goodison and Walker, 1995). Despite some issues, SWE estimates with accuracies of less than ±15mm have been obtained from passive microwave radiometry in many of the planar regions of Central Canada (Derksen et al, 2003; Derksen et al., 2005), where low forest-cover, dryer snow conditions, and a lack of complex underlying topography make assessment of radiometric data more accurate (Goodison and Walker, 1995). In general, algorithm development for SWE retrieval from space-borne passive microwave brightnesses temperatures in Canada has focused on the open prairies regions of central Canada (Wulder et al., 2007; Goodison and Walker, 1995; Walker and Goodison, 2000). Assessments of algorithm performance in these areas have shown that retrievals over the planar regions of North America are

suitable for large-area climatological analysis (Derksen et al., 2003a, 2003b), though

these estimates tend to systematically underestimate SWE in areas with more complex

interaction with vegetation (Derksen et al., 2003; Walker and Silis, 2002).
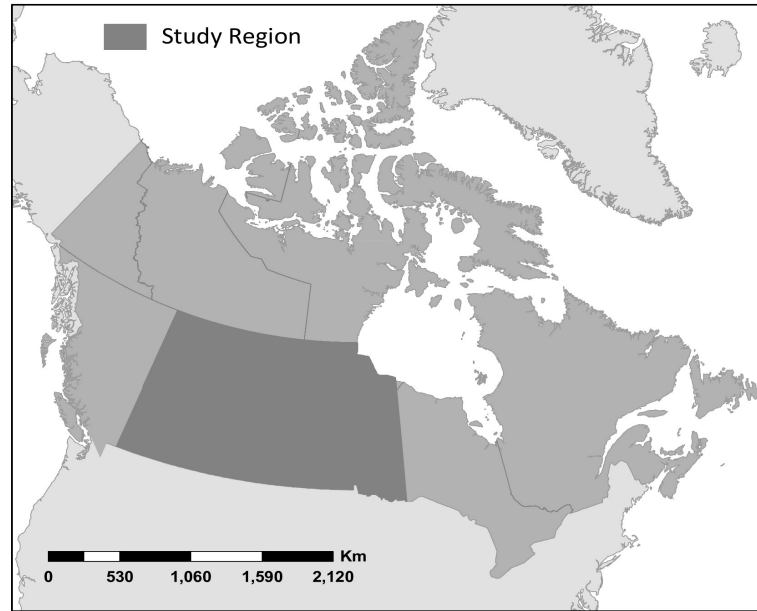
Figure 3.1: Study region encompasses the Canadian prairies, extending from approximately -120o to -90o West, and from 60o to 50o North.

3.3.2.   Study area and data

This study will be constrained to the Canadian prairies (Figure 3.1), extending from

approximately -120º to -90º West, and from 60º to 50º North. SWE estimates in this area

have high accuracy, and are based on brightness temperatures (in Kelvin) acquired by the

SSM/I passive microwave radiometer on-board the Defense Meteorological Satellite

Program (DMSP) F8, F11 and F13 satellites. We use brightness temperatures from a

single orbit of the SSM/I passive microwave radiometer provided in the Equal Area

Scalable Earth Grid (EASE-Grid) format (see Armstrong and Brodzik, 1995) from the

National Snow and Ice Data Center (Knowles et al, 1999; Armstrong et al, 1994). Brightness temperatures represent the difference between the 37 and 19 GHz vertically polarized channels, and in all cases, data collected during the morning overpass were used for analysis to reduce errors induced by afternoon snow melt (Derksen et al, 2000). The 37 and 19 GHz vertically polarized channels are the conventional frequencies used to estimate SWE in most algorithms (Goodison, 1989), making it is possible to reduce data errors induced by algorithm issues, and excess data manipulation and estimation by using brightness temperature differences as a proxy for actual SWE estimates. Values are represented using 25 by 25 kilometer pixels, and the current analysis focuses on data obtained daily from the beginning of the SSM/I satellite record (1987), to 2006. For a review of methods for SWE estimation and algorithm development, see Goodison and Walker (1995), Walker and Goodison (2000), and Pietroniro and Leconte (2000).

Atmospheric effects, sensor errors, and the properties of the snow pack on any given day will cause local variations in the time-series of detected passive microwave signals. For example, passive microwave derived brightness temperatures used for extracting SWE are typically within ±15 mm of actual SWE in the open prairie regions of North America (Derksen et al. 2003; Derksen et al. 2005); however, consistent underestimation is a problem in many forested areas, and is likely the result of vegetation influencing on microwave emission and scatter (Derksen et al. 2005, Foster et al. 1991). In addition, brightness temperature fluctuations due to snow melt occur throughout the SSM/I time-series, and are most prevalent during the weeks preceding the major snow melt events (spring snow melt). These fluctuations in the data can be attributed to irregularities

induced by a wet snow pack (Walker and Goodison 2000; Derksen et al. 2000), and are not reflective of the actual SWE occurring at a particular site.

An ancillary data set used to assess the nature of SWE Regimes are ecoprovinces. Ecoprovinces are ecological management units based on terrestrial characteristics were developed as part of the National Ecological Framework of Environment Canada (Rowe and Sheard 1981; Wiken 1986; Wiken et al 1996). Ecoprovinces are largely based on characterizing major assemblages of structural or surface forms and faunal realms, as well as vegetation, hydrology, soil, and macro climates (Marshall et al. 1998). They were developed as part of an ecological framework to address the environmental concerns of the Commission for Environmental Cooperation (CEC) by Canada, Mexico and the United States (Marshall and Schut 1999). Subsequently, ecoregions are characterized by distinctive large order landforms, or assemblages of regional landforms, small order macro- or meso-climates, vegetation, soil, and water features (Wiken et al. 1996). These ecological units are useful for describing the major driving factors of an ecosystem, and as such are useful for conservation planning and analysis (Kerr and Deguise 2004). We use these classifications as the baseline ecological management units with which to compared our derived SWE regimes. For a review of the history of ecological regionalization in Canada, see Bailey et al. (1985). Descriptions, background, and basic ecosystem concepts from the Ecological Framework of Canada are available at <http://www.ec.gc.ca/soer-ree/English/Framework/default.cfm>

3.4. Methods

The annual and inter-annual temporal patterns of SWE are determined by novel application of existing spatial and temporal analysis methods to a long-term, spatially-referenced dataset on SWE. For the current analysis, daily SWE brightness temperature differences are obtained for each 25 km by 25km grid cell in the dataset. Analysis is carried out over 19 years, providing a time-series of approximately 6,935 days of SWE estimates per grid cell (total of 5325 grid cells). As SWE is a seasonal variable, these time-series form cyclic SWE accumulation/melt curves. Smoothing functions are fit to the observed data, and the temporal components of each time-series' are used to generate temporal metrics by treating each grid cell within the study region as a separate cyclic time-series. Several temporal metrics are integrated into a hierarchical, multivariate classification algorithm. The results of the classification are used to delineate SWE regimes, providing a means for defining SWE management units for both ecological and anthropogenic processes.

3.4.1. SWE curve fitting procedure

In order to capture important patterns in SWE time-series, various smoothing methods to reduce data errors are used in practice. These methods include the use of weekly (e.g. Derksen et al. 2000; Derksen et al. 2002; Derksen et al. 2000), monthly (e.g. Derksen et al. 2005), and yearly (e.g. Wulder et al. 2007) running means. In addition, spatial averaging of SWE values has been used to reduce variability, as well as examine relationships between SWE and atmospheric circulation (Derksen et al. 2000. These methods rely on data-reduction to correct for problems induced by the atmosphere, temperature, and the snow pack itself, and may over generalize important annual or inter-

annual fluctuations in the SWE time-series. In addition, these methods do not take into account the inherent properties of passive microwave derived SWE data, such as systematic and non-systematic underestimation of SWE.

One method which has been used in research on remotely sensed vegetation indices uses splines in a recursive setting to fit a continuous model to Normalized Difference Vegetation Index (NDVI) data (Bradley et al. 2007; Hermance et al. 2007; Hermance, 2007). By recursively fitting high order splines to the data, the effects of drop-outs and spurious fluctuations in the data are reduced, and the local variation in vegetation temporal cycles captured. Applying a similar approach to SWE data should reduce problems associated with the effects of snow pack inhomogeneities and erroneous fluctuations in the brightness temperature satellite record.

Smoothing splines are an indirect smoothing method based on penalized least squares, and define a continuous function using a series of polynomials fitted over adjacent time intervals along the SWE time-series (Green and Silverman, 1994). The function is constrained such that both the first and second derivatives, as well as the function itself are continuous at the intersections of the temporal intervals. Thus, for a given time-series y, a smoothing spline is used to model the data as

$$y_i = f(t_i) + \epsilon_i,$$

where f is some unknown smooth function of t, and ϵ represents independent and identically distributed errors. The estimate of f, $\hat{f}$ is chosen so that it minimizes

$$\sum_{i=1}^{n} (y_i - f(x_i))^2 + \lambda \int (f''(t))^2 dt .$$

The smoothing parameter λ must be specified, and is used to control the exchange

between observed data fidelity and curve smoothness, and represents the rate of exchange

between the residual error, or data fidelity,

$$\sum_{i=1}^{n} (y_i - f(x_i))^2 ,$$

and the roughness of the curve

$$\int (f''(t))^2 dt ,$$

In the current example, λ is selected using generalized cross-validation. This is a

common method for selecting smoothing parameters, and is simply a modified form of

the usual cross-validation (see Green and Silverman 1994; Craven and Wahba 1979).

Due to the large variability in inter-annual SWE temporal characteristics, fitting a

harmonic average annual base model to the SWE data, as in Hermance et al. (2007) and

Hermance (2007), proved problematic. As such, both the initial and secondary models in

the recursive spline algorithm applied here are fit using smoothing splines. Given that

SWE brightness temperature returns tend to underestimate the actual about of SWE on

the landscape in some areas (Derksen et al. 2005), we employ a weighted least squares

approximation for the second iteration of the spline fitting procedure in order to

preferentially fit the upper envelope of the data. As in Hermance et al. (2007), residuals

between the initial spline model and the observed SWE values are computed from

$$\Delta d(i) = d_{obs}(i) - d_{pred}(i),$$

Where $d_{obs}(i)$ is the observed SWE values, and $d_{pred}(i)$ is the value predicted by the initial spline model. A Gaussian-type weight is applied to each observed value based on

$$Weight_i := \begin{cases} 0, & |(\Delta d)_i| \geq 15 \\ \exp(-sign(|\Delta d|/w)^2), & |(\Delta d)_i| < 15 \end{cases}$$

where w is a parameter used to control the width of the Gaussian operator, and for the current application is set at 5 brightness temperatures, sign is an operator whose value is -1 for negative Δd and +1 for positive Δd, and the effects of spurious outlying brightness temperature returns (greater than 15 brightness temperature values from initial fitted curve) due to confounding snow properties such as wet snow, were controlled by setting their weights equal to zero. The computed weights are applied to each observed value in the dataset for the second iteration of the spline algorithm, producing a smoothed, continuous, penalized weighted least squares approximation of the SWE temporal signature for each grid cell in the dataset.

3.4.2. Derivation of seasonal temporal metrics

A discrete moving window, with a width based on the observed periodic nature of the SWE time-series' (approximately 365 days), is used to compute the suite of temporal metrics for each SWE season. The temporal components that are computed from the time-series are given in Table 1, and are adapted from Lloyd (1990), Malingreau (1986),

and Reed et al. (1994). For each grid cell, temporal trends are summarized using 12

different temporal metrics, summarized annually (12 metrics X 19 years), and are

represented graphically in Figure 3.2 and will be described below. By computing each

metric for each year in the study period, we are able to investigate inter-annual variability

in the computed metrics.

Table 3.1: Each of the 12 temporal metrics are computed for each grid cell in the study region, for all 18 years of the study period.

Metric	Description	Derivation
SACC	Start of SWE accumulation season	First negative turning point (trough) of the second derivative of the smoothed SWE curve
EMEL	End of SWE melt season	Absolute maximum of the second derivative of the smoothed SWE curve
SMEL	Start of SWE melt season	Absolute minimum of the second derivative of the smoothed SWE curve
TINS	Time integrated SWE (Sum of SWE)	Area under the smoothed SWE curve between the SACC and EMEL
RACC	Rate of SWE accumulation	Mean value of the first derivative during accumulation season
RMEL	Rate of SWE melt	Mean value of the first derivative during melt season
SLEN	Length of SWE season	Time between SACC and EMEL
TMAX	Timing of maximum SWE	Time of maximum value of the smoothed SWE curve between SACC and EMEL
TMIN	Timing of minimum SWE	Time of minimum value of the smoothed SWE curve between SACC and EMEL
MAXS	Maximum SWE value	Maximum value of the smoothed SWE curve between SACC and EMEL
MINS	Minimum SWE value	Minimum value of the smoothed SWE curve between SACC and EMEL
RNGS	Range of SWE values	Range between MINS and MAXS
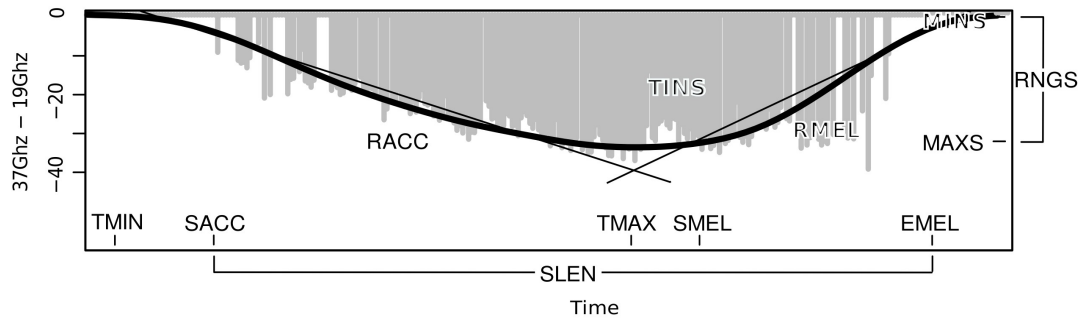
Figure 3.2: Graphical representation of the 12 computed temporal metrics. SACC=Start of SWE accumulation season; EMEL=End of SWE melt season; SMEL=Start of SWE melt season; TINS=Time integrated SWE (Sum of SWE); RACC=Rate of SWE accumulation; RMEL=Rate of SWE melt; SLEN=Length of SWE season; TMAX=Timing of maximum SWE; TMIN=Timing of minimum SWE; MAXS=Maximum SWE value; MINS=Minimum SWE value; RNGS=Range of SWE values.

Derivation of the temporal metrics is based on the properties of the smoothed curve used to represent the SWE values through time. To derive the start of the SWE accumulation season(SACC), we use the first negative turning point (trough) of the second derivative of the smoothed SWE curve within each discrete temporal window (Figure 3.3c). Similarly, to compute the start (SMEL)and end (EMEL) of the SWE melt season, we use the absolute minimum and maximum second derivative of the smoothed SWE curve within each discrete temporal window respectively (Figure 3.3c). The start and end of melt season for the current analysis represents the start and end of the major melt events, as opposed to early-season melt due to fluctuating temperatures, or freeze-thaw interactions.

The time integrated SWE (TINS), or seasonal sum of SWE values, is the area under the

smoothed SWE curve between the start of the accumulation season and the end of the melt period (Figure 3.3a). In addition, the values of the first derivative of the smoothed spline curve are used to compute both accumulation (RACC) and melt (RMEL) rates (Figure 3.3b). For the current analysis, rates are defined as the mean value of the first derivative during each subsequent season. In other words, the SWE accumulation rate is the average slope of the smoothed spline curve during the accumulation season, and the SWE melt rate is similarly defined for the melt season.

The remaining 6 temporal metrics are derived directly from the smoothed SWE curve, and are based on the previously computed metrics (Figure 3.3a). The length of the SWE season (SLEN) is derived by the time from the start of the SWE accumulation season to the end of the SWE melt period. Season length is then used to constrain the values and dates of the maximum (TMAX, MAXS) and minimum (TMIN, MINS) SWE. Building on these metrics, the SWE range is the range between minimum and maximum SWE in a given year (RNGS).

It is important to note that the metrics presented here may not necessarily represent the true SWE conditions on the ground surface, but rather are a representation of the SWE temporal dynamics (Bradley et al. 1994). The exact date, value, and characteristic that an individual temporal metric is attempting to capture may not be precise, given the spatial resolution provided by this dataset; however, it does provide an indication of the spatial-temporal dynamics, and differences in the temporal dynamics of SWE.
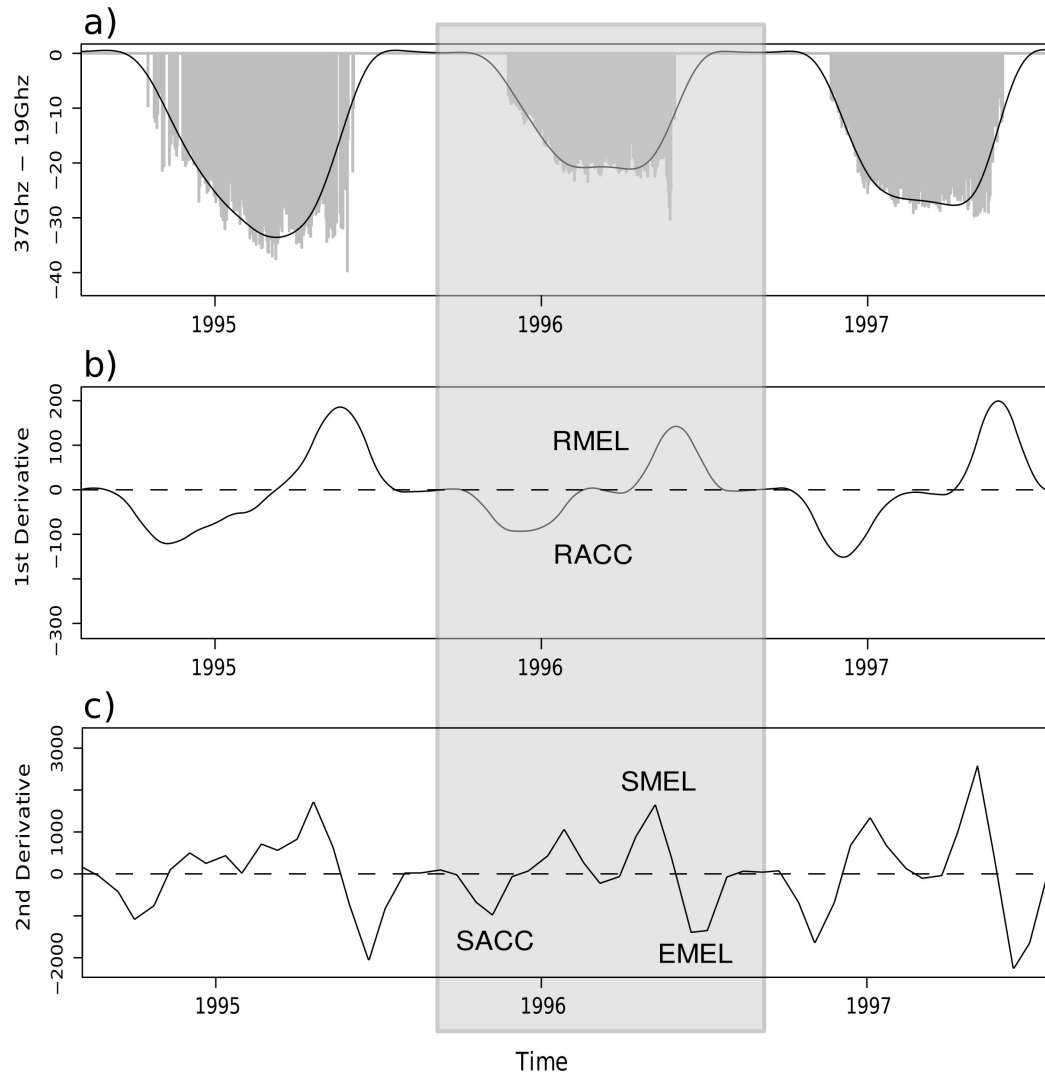
Figure 3.3: Derivation of the 12 temporal metrics. Metrics are based on the properties of the smoothed curve used to represent the SWE values through time, including the values of the curve itself, as well as the 1st and 2nd derivatives. Grey shaded area represents one discrete temporal window.

3.4.3. Analysis of temporal metrics

In order to reduce data redundancy caused by correlated temporal metrics and aid

interpretability of results, we limit the number of temporal metrics used in the final

hierarchical cluster analysis based on ecological significance and data characteristics.

Ecological significance of the three metrics retained will be discussed below and include:

(a) the coefficient of variation in SWE melt rates (CMR), providing a perspective on

temporal changes in SWE due to climate; (b) the annual maximum SWE (AMS),

indicating the water storage levels along the time-series; and (c) the coefficient of

variation in time integrated SWE (CTS), which is the sum of all measured SWE values,

and represents the variability in snow pack development over the time series. Using the

full 19 year time-series, we compute the mean (AMS), and CV (CMR and CTS) for the

three temporal metrics and ensured that these metrics were uncorrelated using a standard

correlation matrix. As suggested by Everitt (1974), metric values were standardized prior

to integration via hierarchical cluster analysis.

Snow accumulation and melt rates, represented by CMR, have important ecological

consequences, and strongly influence the timing and length of the SWE season. This in

turn is an important control of seasonal vegetation growing patterns (e.g. Walker et al.

1999; Kudo 1991; Walther et al. 2002; McCarty 2001), and animal habitats (e.g. Karl et

al. 1993). From a climate change perspective, significant changes in the rates of snow

melt may cause a shift in the overall snow cover season, a change in the total duration of

the snow season, or a change in overall snow seasonality. Characterizing variability of

SWE melt rates is therefore important for identifying the response of snow cover and

SWE to climate change. This makes CMR a useful variable to consider when distinguishing regional variations in SWE temporal characteristics, as regional variations in CMR will highlight areas differentially impacted by changes in temperature and humidity induce by changing climate conditions.

While the variability of SWE melt events is important for characterizing changes induced by climate change, it does not address water storage, which is important for flood forecasting, water resource management , and hydroelectric power generation (Pulliainen and Hallikainen 2001; Chang et al. 2003). Water storage is represented by the AMS metric, and is an important indicator of spring runoff which controls surface water availability for a region. Regardless of the rate and amount of snow accumulation and precipitation over a region, variations in the capacity of an area to store water will have major consequences for the surrounding regions, and will ultimately highlight major differences in SWE regimes. The CTS metric provides an indication of the variability in characteristics of snow pack development and a means to estimate SWE seasonal activity. While it may be difficult to directly determine whether a region experienced steady or varied snowfall events, or whether there are changes over time in the nature of snowfall events (i.e., an increase in extreme snowfall events or trace precipitation events), these characteristics will be indirectly reflected in CTS.

3.4.4. Hierarchical cluster analysis

Hierarchical cluster analysis has been used for a range of applications, including ecological analyses (McKenna 2003; Nemec and Brinkjurst 1988), hydrological

regionalization (Rao and Srinivas 2006; Poff 1996), and climate zone delineation (Gong

and Richman 1995; Unal et al. 2003). Cluster analysis in its most general form is a

method for identifying patterns within multivariate data (Sneath and Sokal 1973;

Kaufman and Rousseeuw 1990). More specifically, hierarchical cluster analysis involves

recursively grouping similar objects based on multivariate attributes into groups. There

are a range of methods for assessing similarity of objects or groups with cluster analysis,

and different approaches will highlight different aspects of a dataset (McKenna 2003;

Johnson, 1976). Measures of similarity based on Euclidean (square) distances in attribute

space are common in the ecological literature (e.g. Fovell and Fovell 1993; Gong and

Richman 1995; Nemec and Brinkhurst 1988), and as such, we compute similarity of grid

cells based on Euclidean distance in the three temporal metrics (CMR, AMS, and CTS).

In addition to the measure of (dis)similarity, hierarchical cluster analysis requires

linkages between previously formed clusters to be measured and assessed for merging.

This in effect dictates how higher-level fusions are executed (McKenna 2003). For the

current analysis, we use an average linkage agglomerative clustering algorithm, which

computes the distance between two clusters as the average measured distance between all

pairs of objects, in this case grid cells, between the two clusters. For our dataset,

consisting of $n = 3$ temporal metrics, we generate a similarity matrix $\boldsymbol{D}$ using

$$d_{ij} = \sqrt{\sum_{k=1}^{n} (x_{ik} - x_{jk})^2} \; ,$$

where d_{ij} is the Euclidean distance in attribute space between grid cell i and j, $j{\neq}i$. From

this, linkages between clusters are assessed based on

$$d_{lm} = \frac{1}{N_l N_m} \sum \sum d_{ij} \, ,$$

where d_{ij} is the Euclidean distance in attribute space between grid cell i in cluster l and grid cell j in cluster m, and N_i and N_m are the number of grid cells in clusters l and m respectively. The cluster grouping that minimizes d_{lm} is then used to group the clusters. This process is performed recursively until a single cluster remains, providing a hierarchical grouping of grid cells based on their associated temporal metrics. As the clusters are grouped to form increasingly larger clusters, a hierarchical grouping tree known as a dendrogram is generated, providing a visual representation of the hierarchy of SWE clusters at various scales. Each node in the dendrogram occurs at a specified height, which is defined as the linkage distance between the two children clusters. The dendrogram is used to assess the relevance of the clusters, allowing us to reject clusters which contain very few grid cells or clusters which contain grid cells that are spatially dispersed.

Once the dendrogram has been formed, we must distinguish between clusters that reflect relationships of the phenomena represented by the data, and those generated as a result of random effects and/or data uncertainties (Nemec and Brinkhurst 1988; McKenna 2003). There have been many methods proposed which use the statistical properties of the data to assess significance of clusters (Smith and Dubes 1980; McKenna 2003; Milligan and Cooper 1985; Piller, 1999). One such method employs bootstrap resampling to assess the stability of detected clusters (Hennig 2007; McKenna 2003; Efron et al. 1996; Felsentein 1985). Bootstrap resampling (Efron 1979) applied to hierarchical cluster analysis has

been used in a number of analyses attempting to assess the appropriateness of a particular

hierarchical arrangement (Hennig 2007; Ellis et al. 1991; Pillar 1999; McKenna 2001;

Kerr and Churchill 2001). In its most basic form, bootstrap resampling for hierarchical

cluster analysis involves generating a number of random 'bootstrap samples' from the

original dataset, and creating bootstrap replicates of the dendrogram by applying the

hierarchical cluster analysis to the bootstrap samples. These dendrogram replicates are

each compared with the initial hierarchical assemblage, and significance is based on the

proportion of dendrogram replicates that are similar to the initial dendrogram. For a

comprehensive review of methods for bootstrap hierarchical cluster analysis in general,

see Efron et al. (1996) and Nemec and Brinkhurst (1988).

Bootstrap resampling has been refined to enable the stability of the hierarchical

classification to be determined by considering the stability of each individual cluster

(Hennig 2007). For example, a number of bootstrap replicates of the initial dendrogram

are created as above, and for each cluster in the initial dendrogram, the most similar

cluster in each bootstrap replicate is found using the Jaccard coefficient (Jaccard 1901) as

a measure of similarity. The level of similarity is recorded, and cluster stability for each

cluster is assessed based on the mean similarity over all resampled data sets. This is done

to ensure that only meaningful clusters are identified, leaving spurious clusters to be

assessed individually by the analyst. In the current example, these clusters can be

combined with the geographically nearest valid clusters to maintain spatial contiguity of

observed clusters, reducing the effects of spurious clusters on the final SWE regime

delineation. An additional benefit is that relative to other bootstrap approaches,

determining the 'optimal' number of clusters via this method requires fewer bootstrap replications to produce valid results (Hennig 2007). As such, we use Hennigs cluster-wise assessment of stability to determine the 'optimal' number, and configuration of SWE regimes across the Canadian Prairies. By constraining the number of possible clusters to be between 15 and 25, we select the final hierarchical dendrogram based on the cluster arrangement that maximizes the proportion of stable clusters, using a mean Jaccard coefficient cutoff of 0.5 (Hennigs, 2007).

3.4.5. Comparison with ecoprovinces

In order to assess the differences between the hierarchically defined SWE regimes and current ecological management units (based on terrestrial ecoprovinces), we examine the spatial correspondence between these two landscape partitioning methods. Comparing units defined using winter and summer conditions will provide an indication of how well winter processes are represented by traditional ecological management units and may provide insights for improving winter based modeling and research efforts. At the current scale of analysis, ecoprovinces represent the most appropriate comparison with SWE regimes, as they are designed to capture major structural assemblages and macro-climates (Marshall et al. 1998), which both tend to have a strong influence on snow deposition and accumulation. The comparison of SWE regimes with ecoprovinces is done by intersecting the boundaries of both regions, and considering the distribution of values on a pixel-by-pixel basis. We then examine the variability in winter conditions for each ecoprovince, highlighting ecoprovinces with a relatively high and/or relatively low number of different SWE regimes within its boundaries.

3.5. Results

3.5.1. Temporal metrics

The spatial and frequency distributions for the three temporal metrics (CMR, AMS, and CTS) are given in Figure 3.4a, 3.4b, and 3.4c). Over the study region, CMR ranges from approximately 23.80 cm, to 0.04 cm per day, with the bulk of the study region experiencing melt rates of approximately 10.32 cm per day. Regional variations in the variability of CMR highlights a large area towards the south-central portion of the study region where melt rates are highly variable relative to the mean melt rate for the entire study region (Figure 3.4A). On the western side of this region, there is an abrupt change to more stable CMR conditions, whereas the portion of the study area to the east of this highly variable region experiences slower transitions to more stable conditions. Conversely, the northern portion of the study area is largely characterized by relatively stable CMR throughout the measured time-series.

For AMS, differences in brightness temperatures range from -43.84 Tb to -7.98 Tb, corresponding to approximately 92.85 to 0.00 mm. Values are normally distributed, with a mean of -22.04 Tb. Regions of low AMS generally occur in the south-west portion of the study region (Figure 3.4B), and there is a general trend of increasing AMS towards the north-east. Two bands of relatively high AMS occur over the central and northern reaches of the study region, both with a north-east to north-west orientation. These bands correspond with regions of relatively high annual precipitation, and long, cold winters with continuous snow cover. Conversely, regional trends are less pronounced with CTS than with AMS, with smaller patches of high variability occurring throughout the central

portion of the study region (Figure 3.4C). The frequency distribution of values for CTS

is slightly skewed (skewness = 0.88), and values range from 0.04 to 0.7 (Figure 3.4c). In

general, large CTS values occur over regions of high AMS. However, these large values

also appear to be relatively stable, occurring to a large degree over the stable band of CTS

in the north-east portion of the study region, west of Hudsons Bay. Regions of high

values occur at the base of the Rocky Mountains, in some cases extending towards

central Alberta and across the international boarder to the south.
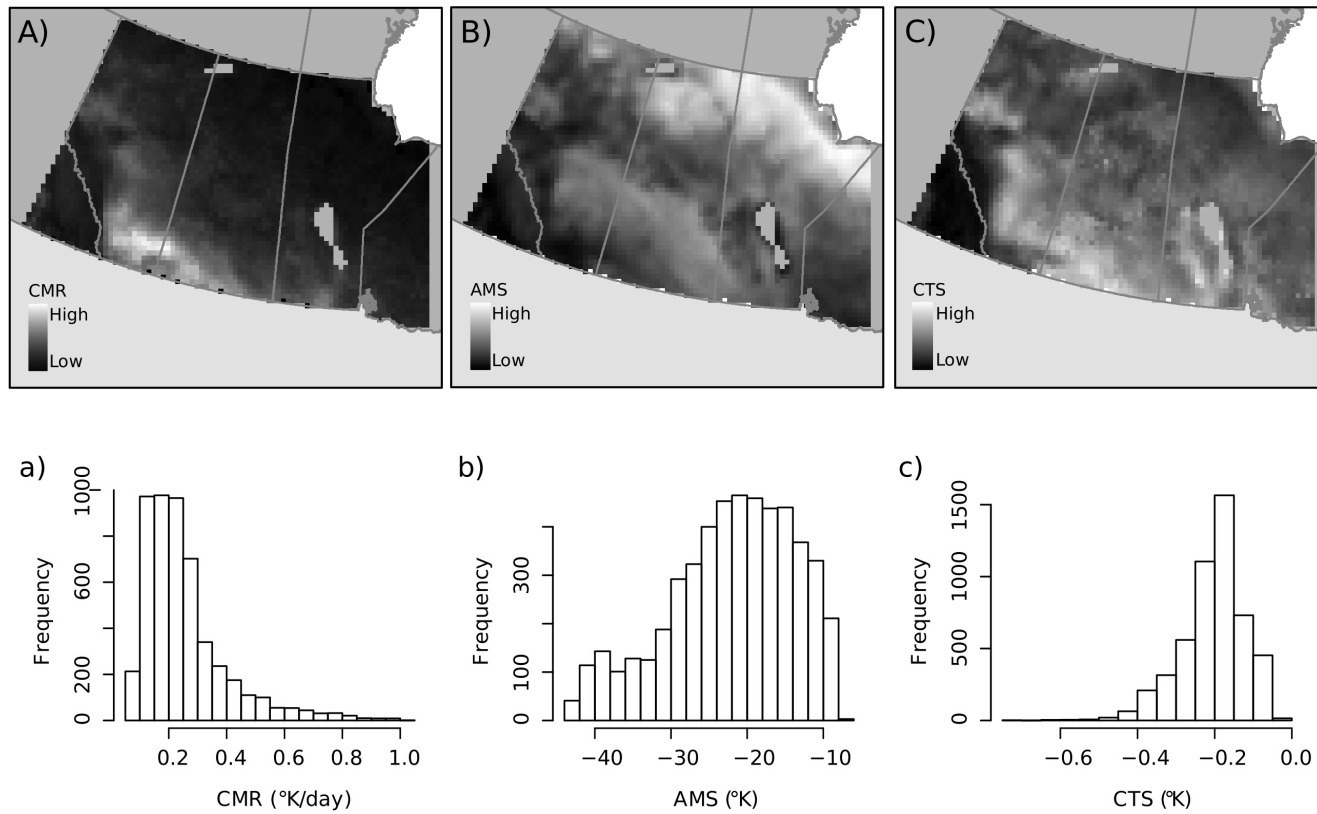
Figure 3.4: The spatial and aspatial distribution of values for the three temporal metrics; Annual mean maximum SWE (A, a), Variability in SWE melt rates (B, b), and Variability in SWE seasonal activity (C, c).

3.5.2.   Hierarchical cluster analysis

The hierarchical cluster arrangement with the highest proportion of stable clusters for the current analysis represents 18 clusters of varying composition and configuration. This arrangement occurs at a clustering height of approximately 1.3 with cluster sizes ranging from 823 to 4 grid cells. All 18 clusters are listed in Table 2, with summary statistics computed over all grid cells located within each cluster for each of the three temporal metrics.

The first two clusters in the hierarchical arrangement are characterized by average levels of variability in terms of SWE melt rates, and relatively low mean maximum SWE. The variability in seasonal SWE activity in these regions is relatively close to the study area mean, though the distribution of values is highly skewed towards less stable conditions. These traits are particularly pronounced in the first cluster, which occupies the lower southeastern slopes of the Rocky Mountains and the western edge of the Alberta Plains, and to a lesser degree, some extremely dry highland regions of the Rocky Mountains.

Clusters located over the open grasslands in the Interior Plains of Canada exhibit an interesting pattern. In general, there is a slow gradient in the values of three temporal metrics as we move from clusters 8 and 9, through 12, 11, 6, and 5 to 15. Clusters 8, 9, and 12 are characterized by some of the highest variability in melt rates across the study area, as well as average variability in SWE seasonal activity, and consistently low maximum SWE values. Conversely, clusters 11 and 6 appear to be part of a transition zone between the high variability in melt rates to the south, and more stable conditions to

the north. This is reflected in the decrease in variability of SWE melt rates, and maximum SWE values towards clusters 5 and 15, where melt rates are once again close to the mean for the entire study region, and maximum SWE tends to be significantly lower than surrounding regions. Variability in SWE seasonal activity throughout these two regions is consistently low, indicating that SWE processes are more stable here.

North of this prairie region is cluster 3, which has the largest cluster area, and includes much of central Canada. Values for all three temporal metrics in cluster 3 are close to the mean for the entire study region. Cluster 3 occupies approximately 22.80% of the overall study region, stretching from south-western Manitoba, all the way to northern Alberta, with an additional branch extending into central Alberta, along the base of the Rocky Mountains. North-west of this central region are three clusters which show strong linear spatial patterns stretching from northern Ontario to northern Saskatchewan, and in some cases as far as northern Alberta. This region is composed of clusters 7, 13, and 16, and is typified by significantly low variability in melt rates, extreme high maximum SWE values, and relatively high levels of variability in SWE seasonal activity. These characteristics are particularly significant in cluster 16, which lies at the northern extreme of the study region.

The remaining 5 clusters (4, 10, 14, 17, 18) each occupy no more than 4.35%of the total study region, for a total coverage of approximately 5.21%. These clusters occur over regions of rapidly changing gradients for all three metrics, and appear to highlight unique SWE regimes. Cluster 14 appears to be unique from all other remaining clusters. This

cluster is characterized by conditions similar to those located over the southern prairie regions, such as increased variability in both melt rates and SWE seasonal activity, with significantly low levels of maximum SWE. Spatially, it occurs as 5 separate regions, located along the same linear band as cluster 3. These regions include two larger domains which occur over south-eastern Ontario, one region west of Lake Winnipeg, and two smaller regions in central Saskatoon and northern Alberta respectively. Cluster 14, along with clusters 11 through 18, form a unique grouping of grid cells based on their configuration of the three temporal metrics, and were not joined with the remaining clusters until a grouping height of 3.06 in the hierarchical cluster analysis.

Table 3.2: Summary of temporal metrics for each hierarchical cluster.

Cluster	Metric	Mean	Median	StdDev	Min	Max	Cluster	Metric	Mean	Median	StdDev	Min	Max
1	CMR	0.22	0.22	0.04	0.12	0.33	10	CMR	0.61	0.60	0.05	0.54	0.70
	AMS	-11.29	-11.62	2.10	-15.97	-6.75		AMS	-14.71	-14.25	1.42	-17.77	-13.27
	CTS	-0.08	-0.07	0.03	-0.18	-0.04		CTS	-0.29	-0.29	0.02	-0.31	-0.25
2	CMR	0.39	0.39	0.02	0.34	0.46	11	CMR	0.70	0.69	0.07	0.56	0.86
	AMS	-12.35	-12.87	2.89	-16.26	-7.14		AMS	-16.69	-16.55	1.78	-21.11	-12.50
	CTS	-0.18	-0.19	0.04	-0.25	-0.11		CTS	-0.39	-0.39	0.03	-0.48	-0.32
3	CMR	0.25	0.24	0.04	0.15	0.37	12	CMR	0.94	0.94	0.04	0.86	1.02
	AMS	-17.04	-17.20	2.59	-23.46	-10.47		AMS	-12.33	-12.06	1.25	-14.68	-10.32
	CTS	-0.20	-0.20	0.03	-0.26	-0.13		CTS	-0.34	-0.35	0.04	-0.40	-0.28
4	CMR	0.25	0.25	NA	0.25	0.25	13	CMR	0.14	0.13	0.03	0.08	0.24
	AMS	-16.57	-16.57	NA	-16.57	-16.57		AMS	-32.05	-32.02	3.03	-38.36	-25.50
	CTS	-0.07	-0.07	NA	-0.07	-0.07		CTS	-0.18	-0.18	0.03	-0.26	-0.11
5	CMR	0.40	0.40	0.04	0.31	0.54	14	CMR	0.29	0.29	0.03	0.22	0.41
	AMS	-22.20	-22.70	2.58	-26.98	-13.90		AMS	-14.92	-15.25	1.85	-19.27	-9.91
	CTS	-0.28	-0.29	0.03	-0.34	-0.21		CTS	-0.28	-0.27	0.03	-0.34	-0.24
6	CMR	0.47	0.48	0.07	0.29	0.59	15	CMR	0.28	0.28	0.04	0.17	0.37
	AMS	-20.25	-20.63	2.70	-24.80	-11.08		AMS	-25.07	-25.67	2.79	-29.75	-17.34
	CTS	-0.35	-0.35	0.02	-0.42	-0.31		CTS	-0.26	-0.26	0.02	-0.33	-0.20
7	CMR	0.16	0.15	0.03	0.09	0.26	16	CMR	0.10	0.10	0.01	0.07	0.13
	AMS	-23.31	-23.33	2.03	-28.87	-18.46		AMS	-40.04	-39.85	1.54	-43.84	-37.11
	CTS	-0.20	-0.20	0.03	-0.27	-0.14		CTS	-0.16	-0.16	0.02	-0.22	-0.11
8	CMR	0.61	0.59	0.07	0.49	0.77	17	CMR	0.41	0.42	0.03	0.37	0.45
	AMS	-10.15	-9.84	1.39	-13.01	-7.99		AMS	-15.16	-15.96	2.92	-19.43	-11.65
	CTS	-0.18	-0.17	0.03	-0.24	-0.14		CTS	-0.43	-0.43	0.02	-0.48	-0.40
9	CMR	0.82	0.83	0.05	0.72	0.91	18	CMR	0.52	0.52	0.02	0.50	0.55
	AMS	-10.34	-10.17	1.26	-13.12	-8.63		AMS	-11.48	-11.46	0.58	-12.12	-10.88
	CTS	-0.24	-0.24	0.02	-0.30	-0.21		CTS	-0.50	-0.49	0.02	-0.53	-0.49

Table 3.3: Thematic summary of the hierarchical cluster analysis results by ecoprovince; Values represent the percentage composition of each of the ecoprovinces in terms of the 18 clusters. Note: percentages do not necessarily add to 100% due to lakes, and other water bodies.

Eco-province										Clusters								
	1	2	3	4	5	6	7	8	9	10	11	12	13	14	15	16	17	18
4.3	0	0	31.31	0	0	0	33.33	0	0	0	0	0	33.33	0	1.01	0	0	0
5.1	0	0	1.09	0	0	0	9.06	0	0	0	0	0	40.22	0	0.72	48.19	0	0
6.1	0	0	11.69	0	0	0	45.86	0	0	0	0	0	39.94	0.15	1.18	0.74	0	0
6.2	0	0	59.4	0	0	0	18.05	0	0	0	0	0	0	18.8	2.26	0	0	0
6.5	0.84	0	37.82	0	3.36	6.72	0	0	0	0	0	0	0	42.86	0	0	2.52	1.68
9.1	31.76	12.16	37.16	0	6.76	5.41	0	2.03	0	0	0	0	0	0.68	0	0	0	0
9.2	0.28	0.84	52.88	0	12.52	6.33	6.33	0	0	0.14	0	0	1.55	3.94	14.21	0	0	0
9.3	0	0	30.38	0	4.43	10.13	8.23	0	0	0	0	0	0	16.46	25.32	0	0	0
10.1	0	0	0	0	14.52	46.77	0	0	0	0	14.52	0	0	0	0	0	9.68	0
10.2	0	0	0	0	44.91	11.93	0.35	1.05	0	1.05	1.75	0	1.4	0	34.04	0	0	0
10.3	0	0	0	0	14.95	23.53	0.25	8.58	5.15	2.94	32.84	4.9	0	0	4.17	0	0	0
14.3	39.47	28.95	0	0	0	0	0	0	0	0	0	0	0	0	0	0	0	0
14.4	92.02	0.84	0	0.42	0	0	0	1.26	0	0	0	0	0	0	0	0	0	0
15.1	0	0	1.92	0	0	0	5.77	0	0	0	0	0	42.31	0	9.62	13.46	0	0
15.2	0	0	0	0	0	0	0	0	0	0	0	0	10	0	0	75	0	0

3.5.3. Comparison with ecoprovinces

A pixel-based summary of the variation in SWE regimes by ecoprovince (Figure 3.5) yields the results in Table 3. Upon examining the spatial correspondence between summer and winter partitioning methods, it is clear that there is variability in how well winter processes are represented by the various ecoprovinces. The number of different SWE regimes located within a single ecoprovinces ranges from 2 in the Hudson-James Lowlands (15.2) and Southern Montane Cordillera (14.3), to 10 in the Eastern Boreal Plains (9.3), though the ecoprovinces with very few clusters tended to be located towards the edges of the study region. The largest correspondence in terms of percentage coverage of a single cluster is located over the Northern Montane Cordillera (14.4) ecoprovince, where 92.02% of the ecoregion is captured by cluster 1. Similarly high levels of correspondence occur in the northern portion of the study area, where the Western Boreal Shield (6.1) ecoprovince is covered to a large degree by clusters 7 (45.86%) and 13 (39.94%), and the Western Taiga Shield (5.1) and Western Boreal Shield (15.2) ecoprovinces are able to capture 92.86%of cluster 16, and large portions of cluster 13.

Regions where ecoprovinces have more variability in associated SWE regimes, occur towards the central and southern portions of the study region. Despite the large size and widespread linear spatial patterns of clusters 6, 5, 15, and 3 throughout this central region, the ecoprovinces are unable to capture the major SWE patterns that they represent. For example, both the largest and smallest of these clusters (3 and 6) are spread across 9 different ecoprovinces each. In addition, the Parkland Prairies (10.2) and

Central Grasslands (10.3) ecoprovinces of the Prairies ecozone appear to miss major

SWE spatial-temporal patterns, containing portions of 5 and 9 different clusters

respectively. Several of the smaller ecoprovinces towards the south-western edge of the

study region (10.1, 9.3, 6.2, and 6.5) contain a large number of different SWE clusters as

well, though this is due in part to the larger variability in the spatial arrangement of

clusters in this region.
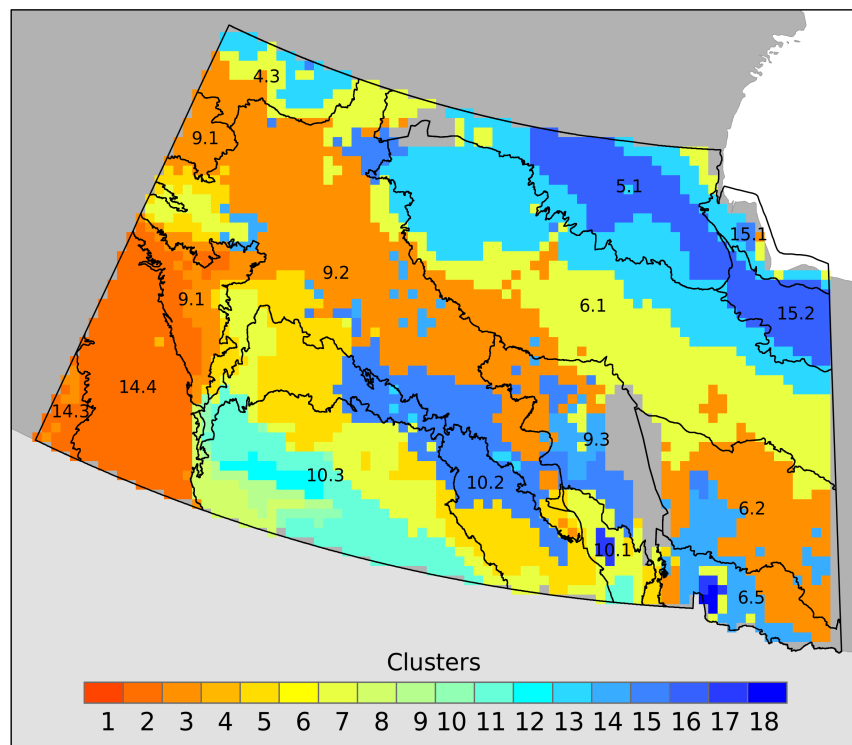
Figure 3.5: Examining the spatial correspondence between hierarchical clusters and ecoprovinces: 4.3=Hay-Slave Lowlands; 9.1=Boreal Foothills; 9.2=Central Boreal Plains; 9.3=Eastern Boreal Plains; 14.4= Columbia Montane Cordillera; 14.3= Southern Montane Cordillera; 10.3=Central Grassland; 10.2=Parkland Prairies; 10.1=Eastern Prairies; 6.1=Western Boreal Shield; 6.2=Mid-Boreal Shield; 6.5=Eastern Boreal Plains; 5.1=Western Taiga Shield; 15.1=Hudson Bay Coastal Plains; 15.2= Hudson-James Lowlands.

3.6.   Discussion

There is a strong spatial component to the distributions of all three temporal metrics presented in this analysis, and this is reflected in the delineation of SWE regimes produced by combining the variability in melt rates, maximum SWE values, and seasonal activity in a hierarchical multivariate setting. The spatial distribution of the three temporal metrics appeared to capture SWE spatial-temporal processes which, to a large degree, are left unobserved using terrestrial ecoprovinces, providing evidence that winter-based processes not capture by current ecological management units.

The hierarchical cluster analysis successfully incorporated different aspects of SWE temporal characteristics to yield distinct geographical regions useful for understanding the general spatial-temporal processes affecting those areas. Emphasis was placed on the temporal relationships within individual regions in order to highlight their unique spatial-temporal attributes. Despite this emphasis, no one SWE regime was completely unique from the overall study region, indicating that there are overarching trends that occur similarly across the entire study region. As a result, similarities in the spatial patterns of SWE regimes were observed, highlighting strong north-west to south-east linear patterns across much of the study region, similar to the accumulation zone described in Derksen et al. (2000b). In addition to this, the Rocky Mountains along the western boarder of the study region have a clear influence on the spatial patterning of SWE across large portions of the prairies.

While in some instances the terrestrial ecoprovinces are able to characterize some of the

variability and trends in the temporal characteristics of SWE, to a large degree these ecological units do not provide sufficient explanation for the observed temporal patterns. This is especially prevalent in the central and southern prairie regions, where high variability in melt rates and seasonal activity, combined with an abundance of SWE, provide highly sensitive regions with strong SWE gradients. This indicates that where SWE is most abundant and variable, current ecological units will be problematic for use when investigating winter based processes. This is corroborated by the comparison between SWE regimes and ecoprovinces, which indicated that clusters with both high and low maximum SWE values over regions of relatively low variability in melt rates and seasonal activity had a higher correspondence than similar regions with relatively high variability.

In some areas, ecoprovinces are more appropriate for assessing winter based processes. Where SWE tends to be low and variability minimal, regions based on spring and summer conditions provide an acceptable representation of winter processes. Examples of this include ecoprovinces along the western extent of the study area, and north of the prairies towards the Boreal Plains and Boreal Shield. In these ecoprovinces correspondence with SWE regimes was high, and ranged between 48.19 and 92.02%. This finding is in line with those found Wulder et al. (2007), in which they discuss a north-west to south-east zone of relatively stable SWE conditions across the boreal forest which tended to be resistant to climate variability through time. According to Derksen et al. (1998c) this zone appears to correspond with the direction of atmospheric airflow based on the 500 mb geopotential height field.

The SWE regimes generated as a result of this analysis should be used as guidelines for developing winter-based management units in conjunction with current ecological classifications. Regions where correspondence is weak, such as in the prairies and southern boreal plains, may warrant reconsideration, or require tailoring for specific modeling, or management applications. Conversely, regions of high correspondence, such as those located west of central Alberta and towards the Hudsons Bay, may be sufficient for examining winter-based processes in their current state.

3.7. Conclusion

The methods presented in this paper provide tools for spatially explicit analysis of long time-series datasets derived from satellite imagery. We utilize methods from time-series analysis, geographic information systems (GIS), ecosystem classification, and remote sensing to provide a unified perspective on the spatial-temporal interactions of SWE. Results are useful for environmental monitoring of SWE and SWE processes, as well as winter-based modeling and research. In addition, the results from this research present opportunities for modeling spatial processes that are year long. For instance, summer processes can be modeled with regions defined based on summer conditions and winter processes modeled using winter based regions, such as SWE regimes. By integrating the two time periods, we are better able to represent processes that occur annually and to better understand the temporal dynamics of many physical processes for which a yearly perspective is needed.

While we have demonstrated unique temporal analysis of spatial data on SWE, this

analysis has implications for other types of spatial-temporal analysis in the natural and

human environments when data are collected at fine temporal resolutions over long time

periods. For example, in the delineation of animal home-ranges, soil and atmospheric

regimes, assessing change and delineating housing markets, as well to derive estimates of

representative scales for general spatial analysis.

4.0 CONCLUSION

4.1.   Discussion and conclusions

The need to understand the long-term spatial and temporal characteristics of snow cover

and SWE is clear. Research has indicated that as the climate continue to warm,

hydrologic processes driven by snow and snow melt will be intensified in most systems

(Maxwell, 1992, 1997). In addition, it has been shown that the spatial and temporal

persistence of snow cover has a significant impact on climate and atmospheric processes

(e.g. Bojariu and Gimeno, 2003; Cohen and Rind, 1991; Barnett et al., 1989). Thus,

climate change research and mitigation depends on the sensitivity of terrestrial snow

cover to atmospheric conditions and overlying air temperatures in order to monitor our

changing environment. Significant changes in snow depth and extent has implications

for many morphological and biological systems, and snow and climate can greatly affect

the timing and spatial distribution of seasonal activities in both plants and animals. The

goal of this research was to characterize regional variations in both spatial and temporal

patterns of SWE, focusing on the need to understand the processes affecting SWE using

long-term analysis of SWE spatial and temporal patterns. We combine two objectives to

reach this goal: 1) examine the relationships between the spatial patterns of SWE, and

land-cover and elevation, and 2) extract relevant snow regimes based on the spatial and

temporal patterns and trends in SWE. In doing so, we extend current methods for time-

series and spatial analysis to SWE research and integrate temporal analysis of time-series

data with methods for characterizing spatial relationships in a novel context.

In Chapter 2.0, measures of spatial autocorrelation were used to identify clusters of

extreme high and low SWE, and the observed spatial patterns were considered through time in order to investigate the variability of these spatial patterns through space and time. We showed that the number of locations having significant spatial autocorrelation within the study region had increased over the 26 year study period, leading to large clusters of extreme SWE over the Central Grasslands regions, potentially impacting the surrounding Mid-Boreal Uplands regions, and lowland planar regions to the east. Furthermore, the temporal trends and variability in SWE spatial autocorrelation were not strongly associated with current ecological management units, and indeed were found to be largely associated with the regional distribution of elevations. We hypothesized that these associations were likely the result of SWE processes relating to elevation, not captured by the ecoregions, and suggested that consideration of the long-term characteristics of SWE may be better suited to explain the variation in SWE spatial-temporal patterns.

Similarly, in Chapter 3.0, we examined the long-term temporal characteristics of SWE, and identified how they varied across the landscape, in order to delineate geographically distinct SWE regimes. We showed that using metrics to represent the temporal characteristics of SWE, such as variability in melt rates, maximum SWE values, and seasonal SWE activity, in a hierarchical multivariate setting yields SWE regimes with strong spatial components. These SWE regimes were then used to delineate SWE spatial-temporal processes not captured by current ecological management units. We then highlighted regional variations in the ability of current ecological management units to capture the observed SWE regimes, suggesting that the integration of winter-based

processes into current ecological management units is indeed feasible and warranted.

Regions where this type of integration might be beneficial are the southern prairie regions

of Alberta, Saskatchewan, as well as portions of central Manitoba.

4.2.   Research contributions

Long-term monitoring and analysis of the environment will continue to be an important

part of research, management, and mitigation of climate change. As environmental

datasets become increasingly spatially and temporally extensive, new and innovative

methods which deal with long-term, spatially referenced datasets are required. As

geographers, it is important to draw upon the experiences and expertise of others by

integrating methods for spatial, temporal, and spatial-temporal analysis from other fields

to suit our own needs. For example, we have combined methods from spatial statistics,

geographic information systems (GIS), time-series analysis, ecosystems classification,

cluster analysis, and remote-sensing to provide a unique perspective on the spatial-

temporal interactions of SWE. By building on the strengths of each field, and combining

them in a spatially explicit context, we extend these methods to research which has

traditionally emphasized spatial trends of snow cover and SWE over short time periods

(e.g., Derksen et al., 1998a,1998b), or coarse-scale spatial trends (i.e., regional analysis)

of snow cover and SWE over longer time periods (e.g., Brown, 2000; Laternser and

Schneebeli, 2003).

Contributions of this research include the results from our comparison of SWE spatial

autocorrelation with land-cover and elevation in Chapter 2.0. From a technical

perspective, this analysis provides a means of analyzing spatial-temporal data which is both intuitive and informative. We have contributed to the understanding of SWE spatial-temporal processes by highlighting spatial-temporal trends that are both regional and local in scope. This includes the tendency for clustering of SWE to become more spatially constrained through time, as well as the associations between SWE spatial autocorrelation and elevation. Perhaps the most significant contribution of this analysis however, is the identification of a major limitation to the use of current ecological management units for winter based research and analysis. By examining the relationship between variability in SWE spatial autocorrelation and terrestrial ecoregions, we highlighted the need for ecological management units which take into account SWE and other dominant winter processes.

Due to our early recognition of the need for ecological management units that consider winter based processes, we have had the unique opportunity of addressing this need through further research and investigation. This relates primarily to our results from Chapter 3.0, in which we present methods for considering the temporal characteristics of SWE, and use these methods to generate SWE regimes useful for guiding the development and integration of winter based SWE processes into current ecological management units. Furthermore, we locate regional variations in the ability of ecoprovinces to account for SWE temporal characteristics, highlighting areas which would benefit from a winter, or yearlong perspective on the landscape and surrounding ecosystems. This specific contributions of this chapter may have implications for further SWE research specifically, and spatial-temporal analysis more generally.

4.3. General Contributions

There is currently a lack of methods for analyzing the increasing number of datasets

which are extensive in both space and time. Although there have been many proposals

for representing time in GIS and geographical research (e.g., Langran 1990; Langran

1992; Egenhofer and Golledge 1997; Peuquet 2002; Rey and Janikas 2006), there

remains a lack of methods designed explicitly for considering both space and time. As a

result, treatment of space and time in spatial datasets has tended to remain separate, with

many researchers limiting their analysis to either space, or time. Through the course of

this research, we have attempted to reduce this shortcoming in two specific ways: Firstly,

in both Chapter 2.0 and Chapter 3.0 we integrated several methods for analyzing data

both spatially and temporally, highlighting their utility as combined methods for spatial-

temporal analysis. This contribution is designed to address the fundamental need for

explicit spatial-temporal analysis methods. Secondly, throughout the course of this

research, we have developed software which combines the treatment of spatial data in a

GIS using Quantum GIS (QGIS Development Core Team 2008), a free open-source GIS,

with the analytical power of the R statistical package (R Development Core Team 2007),

a free open-source statistical analysis package. The software is designed to bridge the

gap between spatial analysis in GIS, and advance temporal analysis in R. As a result, all

analysis performed in this thesis can be implemented using this newly developed

software: manageR, which is currently freely available for download at

http://www.geog.uvic.ca/spar/carson.

While the methods employed in this research were limited to examining SWE spatial-

temporal characteristics, they could be applied equally well to other types of spatial-temporal analysis in the natural and human environments. In particular, the methods employed in this research may be useful to analysts interested in obtaining objective estimates of animal home-ranges, soil and atmospheric regimes, as well to derive estimates of representative scales for spatial analysis. In addition, this type of analysis will be useful for analyzing the growing number of spatial datasets collected over long time periods, at fine spatial and temporal resolutions.

4.4. Research opportunities

This thesis opens up many exciting research opportunities. For example, there are many areas where the methods employed in both research chapters can be extended and improved. As mentioned in Chapter 2.0, by employing more complex temporal modeling and trend detection techniques, analysts in fields such as water resource management, wildlife management, and climate change research will be able to quantitatively measure complex spatial-temporal interactions through time, developing new knowledge to support management, and mitigation of climate change. Furthermore, the classification method employed in Chapter 3.0 could be further refined in a number of ways. Firstly, the integration of additional variables, such as elevation, temperature, or humidity, into the classification scheme may help to identify finer-scale variations in SWE regimes. Secondly, we emphasize that in order to fully integrate SWE regimes with current ecological management units, a multi-scale, large-area assessment of SWE characteristics is required. A final research opportunity involves the integration of the SWE regimes generated as part of Chapter 3.0 with existing and future ecological management systems.

This will provide a means for summer and winter-based processes to be combined in an effort to better understanding of the temporal dynamics of many physical processes, as well as model processes that occur over multiple seasons.

REFERENCES

Chapter 1.0 References

Barnett, T. P., L. Dümenil, U. Schlese, E. Roeckner, and M. Latif. 1989. The Effect of Eurasian Snow Cover on Regional and Global Climate Variations. *Journal of the Atmospheric Sciences* 46: 661-686.

Barry, R. G. 1985. The cryosphere and climate change. *Detecting the Climate Effects of Increasing CO2*. U.S. Department of Energy, 109-141.

Chang, A. T. C., J. L. Foster, and D. K. Hall. 1990. Satellite sensor estimates of northern hemisphere snow volume. *International Journal of Remote Sensing* 11: 167-171.

Cohen, J., D. Entekhabi. 2001. The influence of snow cover on Northern Hemisphere climate variability. *Atmosphere Ocean* 39: 35-53.

DeFries, R., M. Hansen, and J. Townshend. 1995. Global discrimination of land cover types from metrics derived from AVHRR Pathfinder data. *Remote Sensing of Environment* 54: 209-222.

Derksen, C. and M. McKay. 2006. The Canadian boreal snow water equivalent band. *Atmosphere-Ocean* 44: 305-320.

Derksen, C, M Wulder, E Ledrew, and B Goodison. 1998. Associations between spatially autocorrelated patterns of SSM/I-derived prairie snow cover and atmospheric circulation. *Hydrological Processes* 12: 2307-2316.

Derksen, C., E. LeDrew, A. Walker, and B. Goodison. 2000. Winter season variability in North American Prairie SWE distribution and atmospheric circulation. *Hydrological Processes* 14: 3273-3290.

Gong, G., D. Entekhabi, J. Cohen. 2003. Relative impacts of Siberian and North American snow anomalies on the winter Arctic Oscillation. *Geophysical Research Letters* 30:1848-1851.

Goodison, B. E., and A. E. Walker. 1993. Use of snow cover derived from satellite passive microwave data as an indicator of climate change. *Annals of Glaciology* 17: 137-142.

Hirsch, A., C. T. Cushwa, K. W. Flach, and W. E. Frayer. 1978. Land Classification--Where Do We Go from Here? *Journal of Forestry* 76: 672-673.

Houghton, J. T., Y. Ding, D. J. Griggs, M. Noguer, P. J. van der Linden, X. Dai, Maskell,

K., Johnson, C.A. 2001. *IPCC, 2001: Climate Change 2001: The Scientific Basis. Contribution of Working Group I to the Third Assessment Report of the Intergovernmental Panel on Climate Change*. Cambridge University Press, Cambridge.

Ironside, G. R. 1991. Ecological land survey: Background and general approach. *Guidelines for the integration of wildlife and habitat evaluations with ecological land survey. Wildl. Habitat Can. and Environ. Can., Can. Wildl. Serv., Ottawa, ON* 107.

Johannessen, Ola M., Lennart Bengtsson, Martin W. Miles, et al. 2004. Arctic Climate Change: Observed and Modelled Temperature and Sea-Ice Variability. *Tellus A* 56: 328-341.

Justice, C. O., J. R. G. Townshend, B. N. Holben, and C. J. Tucker. 1985. Analysis of the phenology of global vegetation using meteorological satellite data. *International Journal of Remote Sensing* 6: 1271-1318.

Karl, T. R., P. D. Jones, R. W. Knight, et al. 1993. A New Perspective on Recent Global Warming: Asymmetric Trends of Daily Maximum and Minimum Temperature. *Bulletin of the American Meteorological Society* 74: 1007-1023.

Kudo, G. 1991. Effects of snow-free period on the phenology of alpine plants inhabiting snow patches. *Arctic and Alpine Research* 23: 436-443.

Luce, C. H., D. G. Tarboton, and K. R. Cooley. 1998. The influence of the spatial distribution of snow on basin-averaged snowmelt. H*ydrological Processes* 12: 1671-1683.

Mccarty, John P. 2001. Ecological Consequences of Recent Climate Change. *Conservation Biology* 15: 320-331.

Meir, P., P. Cox, and J. Grace. 2006. The influence of terrestrial ecosystems on climate. *Trends in Ecology & Evolution* 21: 254-260.

Moody, A., and D. M. Johnson. 2001. Land-surface phenologies from AVHRR using the discrete Fourier transform. *Remote Sensing of Environment* 75: 305-323.

Moulin, S., L. Kergoat, N. Viovy, and G. Dedieu. 1997. Global-Scale Assessment of Vegetation Phenology Using NOAA/AVHRR Satellite Measurements. *Journal of Climate* 10: 1154-1170.

Pulliainen, J., and M. Halliskainen. 2001. Retrieval of regional snow water equivalent from space-borne passive microwave observations. *Remote Sensing of Environment* 75:76-85.

Quayle, W. C., L. S. Peck, H. Peat, J. C. Ellis-Evans, and P. R. Harrigan. 2002. Extreme Responses to Climate Change in Antarctic Lakes. *Science* 295: 645.

Räisänen, J. 2001. CO2-Induced Climate Change in CMIP2 Experiments: Quantification of Agreement and Role of Internal Variability. *Journal of Climate* 14: 2088-2104.

Robinson, David A., Kenneth F. Dewey, and Richard R. Heim. 1993. Global Snow Cover Monitoring: An Update. *Bulletin of the American Meteorological Society* 74: 1689-1696 .

Rowe, J. S., and J. W. Sheard. 1981. Ecological land classification: A survey approach. *Environmental Management* 5: 451-464.

Schlesinger, M.E. 1986. Co2-induced changes in seasonal snow cover simulated by the OSU coupled atmosphere-ocean general circulation model. *Snow Watch '85, Glaciological Data, Report* 18: 249-270.

Serreze, Walsh, Chapin, et al. 2000. Observational Evidence of Recent Change in the Northern High-Latitude Environment. *Climatic Change* 46: 159-207.

Tait, A. 1996. Estimation of snow water equivalent using passive microwave radiation data. *Geoscience and Remote Sensing Symposium, 2000. Proceedings. IGARSS 2000. IEEE 2000 International* 4:2005-2007.

Thorn, Colin E. 1978. The Geomorphic Role of Snow. *Annals of the Association of American Geographers* 68: 414-425.

van Vuren, D., and K. B. Armitage. 1991. Duration of snow cover and its influence on life-history variation in yellow-bellied marmots. *Canadian Journal of Zoology* 69: 1755-1758.

Walker, A., and B. Goodison. 2000. Challenges in determining snow water equivalent over Canada using microwave radiometry. *Geoscience and Remote Sensing Symposium, 2000. Proceedings. IGARSS 2000. IEEE 2000 International* 4: 1551-1554.

Walker, M. D., D. A. Walker, J. M. Welker, et al. 1999. Long-term experimental manipulation of winter snow regime and summer temperature in arctic and alpine tundra. *Hydrological Processes* 13: 2315-2330.

Walther, G. R., E. Post, P. Convey, et al. 2002. Ecological responses to recent climate change. *Nature* 416: 389-395.

Wiken, E, E Gauthier, I Marshal, K Lawton, and H Hirvonen. 1996. *A Perspective on Canada's Ecosystems*. Canadian Council on Ecological Areas, Ottawa, Ontario, Canada.

Wiken, E. B. 1986. *Terrestrial ecozones of Canada*. Ecological Land Classification. Environment Canada.

Wulder, Nelson, Derksen, and Seemann. 2007. Snow cover variability across central Canada (1978–2002) derived from satellite passive microwave data. *Climatic Change* 82: 113-130.

Chapter 2.0 References

Anderson, S. P., S. M. White, and B. Alvera. 2004. Evaluation of spatial variability in snow water equivalent for a high mountain catchment. Hydrological Processes 18: 435-453.

Armstrong, R., and M. Brodzik. 1995. An earth-gridded SSM/I data set for cryospheric studies and global change monitoring, Advanced Space Research 16: 10155-10163.

Armstrong, R., K. Knowles, M. Brodzik, and M. Hardman. 1994 – 2002. DMSP SSM/I Pathfinder daily EASE-Grid brightness temperatures, Boulder, CO, National Snow and Ice Data Center. Digital media and CD-ROM.

Barnett, T. P., J. C. Adam, and D. P. Lettenmaie. 2005. Potential impacts of a warming climate on water availability in snow-dominated regions. Nature 438: 303-309.

Barnett, T., L. Dumenil, U. Schlese, E. Roeckner, and M. Latif. 1989. The effect of Eurasian snow cover on regional and global climate variations. Journal of the Atmospheric Sciences 46: 661-685.

Bednorz, E. 2004. Snow cover in eastern Europe in relations to temperature, precipitation and circulation. International Journal of Climatology 24: 591-601.

Boots, B. 2002. Local Measures of Spatial Association. Écoscience 9: 168-176.

Breusch, T., and A. Pagan. 1979. A Simple Test for Heteroscedasticity and Random Coefficient Variation. Econometrica 47: 1287-1294.

Brown, R., A. Walker, and B. Goodison. 2000. Seasonal snow cover monitoring in Canada: An assessment of Canadian contributions for global climate monitoring. 57th Eastern Snow Conference Syracuse, New York.

Brown, R. 2000. Northern Hemisphere snow cover variability and change, 1915-1997. Journal of Climate 13: 2339-2355.

Brown, T., K. Hamza, and A. Xia. 1998. On the Variance to Mean Ratio for Random Variables from Markov Chains and Point Processes. *Journal of Applied Probability* 35:

303-312.

Butler, D., and S. Walsh. 1990. Lithologic, structural, and topographic influences on snow-avalanche path location, Eastern Glacier National Park, Montana. *Annals of the Association of American Geographers* 80: 362-378.

Carroll, S., T. Carroll, and R. Poston. 1999. Spatial modeling and prediction of snow-water equivalent using ground-based, airborne, and satellite snow data. *Journal of Geophysical Research* 104: 19623-19629.

Cliff, A., and J. Ord. 1981, *Spatial processes: Models and applications*. Pion Ltd., London.

Cribari-Neto, F., and S. Zarkos. 1999. Bootstrap methods for heteroskedastic regression models: evidence on estimation and testing. *Econometric Reviews* 18: 211-228.

Defense Mapping Agency, 1986. Defense Mapping Agency product specifications for digital terrain elevation data (DTED) (2nd ed.). Defense Mapping Agency Aerospace Center, St. Louis, Missouri, 26 p.

Derksen, C. and M. McKay. 2006. The Canadian boreal snow water equivalent band. *Atmosphere-Ocean* 44: 305-320.

Derksen, C., E. LeDrew, and B. Goodison. 1998. SSM/I derived snow water equivalent data: the potential for investigating linkages between snow cover and atmospheric circulation. *Atmosphere-Ocean* 36(2): 95-117.

——— 2000. Temporal and spatial variability of North American prairie snow cover (1988-1995) inferred from passive microwave-derived snow water equivalent imagery. *Water Resources Research* 36: 255-266.

——— 2005. Evaluation of passive microwave snow water equivalent retrievals across the boreal forest/tundra transition of western Canada. *Remote Sensing of Environment* 96: 315–327.

Derksen, C., A. Walker, B., Goodison. 2003. A comparison of 18 winter seasons of in situ and passive microwave derived snow water equivalent estimates in Western Canada. *Remote Sensing of Environment* 88: 271–282.

Derksen, C., W. Wulder, E. LeDrew, and B. Goodison. 1998a. Associations between spatially autocorrelated patterns of SSM/I derived Prairie snow cover and atmospheric circulation. Hydrological *Processes* 12: 2307-2316.

——— 1998b. Application of the Getis statistic to hemispheric and regional scale passive

microwave derived snow water equivalent imagery. *Geoscience and Remote Sensing Symposium Proceedings, IGARSS '98. 1998 IEEE International* 2: 977-979.

Dewey, K. 1977. Daily maximum and minimum temperature forecasts and the influence of snow cover. *Monthly Weather Review* 105; 1594-1597.

Essery, R., L. Long, and J. Pomeroy. 1999. A distributed model of blowing snow over complex terrain. *Hydrological Processes* 13: 2423-2438.

Foster, J., D. Hall, A. Chang, A. Rango, W. Wergin, and E. Erbe. 1999. Effects of snow crystal shape on the scattering of passive microwave radiation. *IEEE Transactions on Geoscience and Remote Sensing* 37: 1165-1168.

Getis, A., and J. Ord. 1992. The Analysis of Spatial Association by Use of Distance Statistics. *Geographical Analysis* 24: 189-206.

——— 1996. 'Local Spatial Statistics: An Overview' In *Spatial Analysis: Modeling in a GIS Environment*, (eds) Longley, P. and Batty, M., 261-277. Cambridge: GeoInformation International

Gesch, D., K. Verdin, and S. Greenlea. 1999. New land surface digital elevation model covers the earth. EOS, *Transactions of the American Geophysical Union* 80(6):69-70.

Goita, K., A. Walker, and B. Goodison. 2003. Algorithm development for the estimation of snow water equivalent in the boreal forest using passive microwave data. *International Journal of Remote Sensing* 24(5):1097–1102

Gong, G., D. Entekhabi, J. Cohen, and D. Robinson. 2004. Sensitivity of atmospheric response to modeled snow anomaly characteristics. *Journal of Geophysical Research* 109: D06107.

Goodison, B., and A. Walker. 1993. Use of snow cover derived from satellite passive microwave data as an indicator of climate change. *Annals of Glaciology* 17: 137–142.

——— 1995. Canadian development and use of snow cover information from passive microwave satellite data. In Choudhury, B., Kerr, Y., Njoku, E. and Pampaloni, P. (eds.) *Passive Microwave Remote Sensing of Land-Atmosphere Interactions*. VSP BV, Utrecht, Netherlands, pp. 245–262.

Goodison, B., A. Walker, and F. Thirkettle. 1990. Determination of snow cover on the Canadian prairies using microwave data. *Proceedings of the International Symposium on Remote Sensing and Water Resources, Enschede, The Netherlands*. pp. 127–136.

Goodison, B. 1989. Determination Of Areal Snow Water Equivalent On The Canadian Prairies Using Passive Microwave Satellite Data. *Geoscience and Remote Sensing Symposium, 1989. IGARSS'89. 12th Canadian Symposium on Remote Sensing.*, 3: 1243-1246.

Griffin, P., A. Getis, and E. Griffin. 1996. Regional patterns of affirmative action compliance costs. *The Annals of Regional Science* 30: 321-340.

Hall, D., M. Sturm, C. Benson, A, Chang, J. Foster, H. Garbeil, and E. Chacho. 1991. Passive microwave remote and in situ measurements of Arctic and Subarctic snow covers in Alaska, *Remote Sensing of the Environment* 38: 161-172.

Hollander, M., and D. A. Wolfe. 1999. *Nonparametric Statistical Methods, 2nd Edition*. John Wiley and Sons, Wiley-Interscience, 1999.

Howat, I., I. Joughin, S. Tulaczyk, and S. Gogineni. 2005. Rapid retreat and acceleration of Helheim Glacier, east Greenland. *Geophysical Research Letters*, 32, L22502.

Katz, R., and B. Brown. 1992. Extreme events in a changing climate: variability is more important than averages. *Climate Change* 21: 289-302.

Keller, F., S. Goyette, and M. Beniston. 2005. Sensitivity analysis of snow cover to climate change scenarios and their impact on plant habitats in alpine terrain. *Climate Change* 72: 299-319.

Kendall, M., and J. Ord. 1990, *Time Series, 3rd Edition*. Edward Arnold, London and Oxford University Press, New York, pp 18-21.

Kerr, J.T., and I. Deguise. 2004. Habitat loss and the limits to endangered species recovery. *Ecology Letters* 7: 1163-1169.

Knowles, K., E Njoku, R. Armstrong, and M. Brodzik. 1999. Nimbus-7 SMMR Pathfinder daily EASE-Grid brightness temperatures. *Boulder, CO: National Snow and Ice Data Center. Digital media and CD-ROM.*

Knowles, N., M. Dettinger, and D. Cayan. 2006. Trends in snowfall versus rainfall for the western United States. *Journal of Climate* 19: 4545-4559.

Laternser, M., and M. Schneebeli. 2003. Long-term snow climate trends of the Swiss Alps (1931-99). *International Journal of Climatology* 23: 733-750.

Liu, X., and M. Yanai. 2002. Influence of Eurasian spring snow cover and Asian summer rainfall. *International Journal of Climatology* 22: 1075-1089.

Luce, C., D. Tarboton, and K. Cooley. 1998. The influence of the spatial distribution of snow on basin-average snowmelt. *Hydrological Processes* 12: 1671-1683.

Magnuson, J. 1990. Long-Term Ecological Research and the Invisible Present. *BioScience* 40: 495-501.

Mann, H. B., and D.R. Whitney. 1947. On a test of whether one of two random variables is stochastically larger than the other. *Annals of Mathematical Statistics* 18: 50-60.

Marshall, I., and P. Schut. 1999. A national ecological framework for Canada – overview. *Agriculture and Agri-Food Canada and Ecosystems Science Directorate, Environment Canada, State of Environment Directorate, Ottawa/Hull.*

Marshall, I., E. Wiken, and H. Hirvonen. (Compilers). 1998. Terrestrial Ecoprovinces of Canada. *Ecosystem Sciences Directorate, Environment Canada and Research Branch, Agriculture and Agri-Food Canada, Ottawa/Hull.* Draft Map at 1:7 500 000 scale.

McCabe, G., and D. Legates. 1995. Relationships between 700 hPa height anomalies and April snow pack accumulations in the Western USA. *International Journal of Climatology* 15: 517-530.

Molotch, N. P., M. T. Colee, R. C. Bales, and J. Dozier. 2005. Estimating the spatial distribution of snow water equivalent in an alpine basin using binary regression tree models: the impact of digital elevation data and independent variable selection. *Hydrological Processes* 19: 1459-1479.

Moore, G., and W. Wallis. 1943. Time series significance tests based on sings of differences. *Journal of American Statistical Association* 38: 153-164.

Namias, J. 1985. Some empirical evidence for the influence of snow cover of temperature and precipitation. *Monthly Weather Review* 113: 1542-1553.

NSIDC, 2007. *National Snow and Ice Data Center.* http://nsidc.org/ (Last visited September 2007)

Nolin, A., and J. Dozier. 2000. A hyperspectral method for remotely sensing the grain size of snow. *Remote Sensing of Environment* 74: 207-216.

Olsen, J. R., J. R. Stedinger, N. C. Matalas, and E. Z. Stakhiy. 1999. Climate variability and flood frequency estimation for the upper Mississippi and lower Missouri rivers. *Journal of the American Water Resources Association* 35: 1509-1523.

Ord, J., and A. Getis. 1995. Local Spatial Autocorrelation Statistics: Distributional Issues and an Application. *Geographical Analysis* 27: 286-306.

Pietroniro, A., and R. Leconte. 2005. A review of Canadian remote sensing and hydrology, 1999-2003. *Hydrological Processes* 19: 285-301.

Pulliainen, J., and M. Halliskainen. 2001. Retrieval of regional snow water equivalent from space-borne passive microwave observations. *Remote Sensing of Environment* 75:76-85.

Serreze, M., J. Walsh, F. Chapin, T. Osterkamp, M. Dyurgerov, V. Romanosky, W. Oechel, J. Morison, T. Zhang, and R. Barry. 2000. Observational evidence of recent change in the northern high-latitude environment. *Climatic Change* 46:159–207.

Stafford, J., G. Wendler and J. Curtis. 2000. Temperature and precipitation of Alaska: 50 year trend analysis. *International Journal of Climatology* 67: 33-44.

Tait, A. 1996. Estimation of snow water equivalent using passive microwave radiation data. *Geoscience and Remote Sensing Symposium, 2000. Proceedings. IGARSS 2000. IEEE 2000 International* 4:2005-2007.

Tiefelsdorf, M., and B. Boots. 1997. A note on the extremities of local Moran's Ii and their impact on global Moran's I. *Geographical Analysis* 29: 248-257.

US Geological Survey, 1993*, Digital elevation models, data user guide 5*. Reston, Virginia, 50 p.

Walker, A., and B. Goodison. 2000. Challenges in determining snow water equivalent over Canada using microwave radiometry. *Geoscience and Remote Sensing Symposium, 2000. Proceedings. IGARSS 2000. IEEE 2000 International* 4: 1551-1554.

Wiken, E., D. Gauthier, I. Marshall, K. Lawton, and H. Hirvonen. 1996. A Perspective on Canada's Ecosystems, *Occasional Paper No. 14, Canadian Council on Ecological Areas, Ottawa, ON, Canada*.

Wulder, M., T. Nelson, C. Derksen, and D. Seemann. 2007. Snow cover variability across central Canada (1978-2002) derived from satellite passive microwave data. *Climatic Change* 82: 113-130.

Chapter 3.0 References

Armstrong, R., and M. Brodzik. 1995. An earth-gridded SSM/I data set for cryospheric studies and global change monitoring. Advanced Space Research 16: 10155-10163.

Armstrong, R., K. Knowles, M. Brodzik, and M. Hardman. 1994 – 2002. DMSP SSM/I Pathfinder daily EASE-Grid brightness temperatures. Boulder, CO, National Snow and Ice Data Center. Digital media and CD-ROM.

Bailey, N.T.J. 1985. The Role of Statistics in Controlling and Eradicating Infectious Diseases. The Statistician 34, no. 1: 3-17.

Barnett, T. P., J. C. Adam, and D. P. Lettenmaie. 2005. Potential impacts of a warming climate on water availability in snow-dominated regions. Nature 438: 303-309.

Blasi, C., M. L. Carranza, R. Frondoni, and L. Rosati. 2000. Ecosystem classification and mapping: a proposal for Italian landscapes. Appl. Veg. Sci 3: 233-242.

Bradley, B. A., R. W. Jacob, J. F. Hermance, and J. F. Mustard. 2007. A curve fitting procedure to derive inter-annual phenologies from time series of noisy satellite NDVI data. Remote Sensing of Environment 106, no. 2: 137-145.

Bradley, R.W., F. Cooke, L.W. Lougheed, and W.S. Boyd. 2004. Inferring breeding success through radiotelemetry in the marbled murrelet. Journal Of Wildlife Management 68, no. 2: 318-331.

Brown, R. 2000. Northern Hemisphere snow cover variability and change, 1915-1997. Journal of Climate 13: 2339-2355.

Chang, A.T.C., R.E.J. Kelly, J.L. Foster, and D.K. Hall. 2003. Global SWE monitoring using AMSR-E data. In Geoscience and Remote Sensing Symposium, 2003. IGARSS '03. Proceedings. 2003 IEEE International, 1:680-682 vol.1.

Craven, P., and G. Wahba. 1979. Smoothing noisy data with spline functions: estimating the correct degree of smoothing by the method of generalized cross-validation. Numer. Math 31, no. 4: 377–403.

DeFries, R., M. Hansen, and J. Townshend. 1995. Global discrimination of land cover types from metrics derived from AVHRR Pathfinder data. Remote Sensing of Environment 54: 209-222.

Derksen, C. and M. McKay. 2006. The Canadian boreal snow water equivalent band. Atmosphere-Ocean 44: 305-320.

Derksen, C., A. Walker, B., Goodison. 2003. A comparison of 18 winter seasons of in situ and passive microwave derived snow water equivalent estimates in Western Canada. Remote Sensing of Environment 88: 271–282.

Derksen, C., D. A. Walker, E. Ledrew, and B. Goodison. 2002. Time-series analysis of passive-microwave-derived central North American snow water equivalent imagery. Annals of Glaciology 34, no. 1: 1-7.

Derksen, C., E. LeDrew, and B. Goodison. 1998a. SSM/I derived snow water equivalent

data: the potential for investigating linkages between snow cover and atmospheric circulation. Atmosphere-Ocean 36(2): 95-117.

——— 1998b. Application of the Getis statistic to hemispheric and regional scale passive microwave derived snow water equivalent imagery. Geoscience and Remote Sensing Symposium Proceedings, IGARSS '98. 1998 IEEE International 2: 977-979.

——— 2000a. Temporal and spatial variability of North American prairie snow cover (1988-1995) inferred from passive microwave-derived snow water equivalent imagery. Water Resources Research 36: 255-266.

——— 2005. Evaluation of passive microwave snow water equivalent retrievals across the boreal forest/tundra transition of western Canada. Remote Sensing of Environment 96: 315–327.

Derksen, C., E. LeDrew, Walker, A., and B. Goodison. 2000b. Winter season variability in North American prairie SWE distribution and atmospheric circulation. *57th Eastern Snow Conference, Syracuse, New York, USA.*

Derksen, C., W. Wulder, E. LeDrew, and B. Goodison. 1998c. Associations between spatially autocorrelated patterns of SSM/I derived Prairie snow cover and atmospheric circulation. Hydrological Processes 12: 2307-2316.

Duro, Dennis C., Nicholas C. Coops, Michael A. Wulder, and Tian Han. 2007. Development of a large area biodiversity monitoring system driven by remote sensing. Progress in Physical Geography 31, no. 3 (June 1): 235-260. doi:10.1177/0309133307079054.

Efron, B. 1979. Bootstrap methods: another look at the jackknife. Annals of Statistics 7, no. 1: 1-26.

Efron, B., E. Halloran, and S. Holmes. 1996. Bootstrap confidence levels for phylogenetic trees. Proceedings of the National Academy of Sciences 93, no. 23: 13429.

Ellis, D. V., R. Samoszynski, and A. A. Jones. 1991. Re-analysis of species associational data using bootstrap significance tests. Water, Air, & Soil Pollution 59, no. 3: 347-358.

Everitt, B.S. 1974. Cluster analysis. London: Heinemann

Felsenstein, J. 1985. Confidence limits on phylogenies: an approach using the bootstrap. Evolution 39, no. 4: 783-791.

Foster, J., D. Hall, A. Chang, A. Rango, W. Wergin, and E. Erbe. 1999. Effects of snow crystal shape on the scattering of passive microwave radiation. IEEE Transactions on

Geoscience and Remote Sensing 37: 1165-1168.

Fovell, Robert G., and Mei-Ying C. Fovell. 1993. Climate Zones of the Conterminous United States Defined Using Cluster Analysis. Journal of Climate 6, no. 11 (November 1): 2103-2135 .

Gong, X., and M. B. Richman. 1995. On the Application of Cluster Analysis to Growing Season Precipitation Data in North America East of the Rockies. Journal of Climate 8, no. 4: 897-931.

Goodison, B. 1989. Determination Of Areal Snow Water Equivalent On The Canadian Prairies Using Passive Microwave Satellite Data. Geoscience and Remote Sensing Symposium, 1989. IGARSS'89. 12th Canadian Symposium on Remote Sensing., 3: 1243-1246.

Goodison, B., and A. Walker. 1995. Canadian development and use of snow cover information from passive microwave satellite data. In Choudhury, B., Kerr, Y., Njoku, E. and Pampaloni, P. (eds.) Passive Microwave Remote Sensing of Land-Atmosphere Interactions. VSP BV, Utrecht, Netherlands, pp. 245–262.

Green, P. J., and B. W. Silverman. 1994. Nonparametric Regression and Generalized Linear Models: A Roughness Penalty Approach. Chapman & Hall/CRC.

Grody, N.C., and A.N. Basist. 1996. Global identification of snowcover using SSM/I measurements. Geoscience and Remote Sensing, IEEE Transactions on 34, no. 1: 237-249. doi:10.1109/36.481908.

Hennig, C. 2007. Cluster-wise assessment of cluster stability. Computational Statistics and Data Analysis 52, no. 1: 258-271.

Hermance, J. F., R. W. Jacob, B. A. Bradley, and J. F. Mustard. 2007. Extracting Phenological Signals From Multiyear AVHRR NDVI Time Series: Framework for Applying High-Order Annual Splines With Roughness Damping. Geoscience and Remote Sensing, IEEE Transactions on 45, no. 10: 3264-3276.

Hermance, J.F. 2007. Stabilizing high-order, non-classical harmonic analysis of NDVI data for average annual models by damping model roughness. International Journal of Remote Sensing 28, no. 12: 2801-2819.

Hirsch, A., C. T. Cushwa, K. W. Flach, and W. E. Frayer. 1978. Land Classification-- Where Do We Go from Here? Journal of Forestry 76: 672-673.

Ironside, G. R. 1991. Ecological land survey: Background and general approach. Guidelines for the integration of wildlife and habitat evaluations with ecological land

survey. Wildl. Habitat Can. and Environ. Can., Can. Wildl. Serv., Ottawa, ON 107.

Jaccard, P. 1901. Distribution de la flore alpine dans le bassin des dranses et dans quelque region vasines. Bulletin de la Societe Vaudoise des Sciences Naturelles 37: 241-272.

Johnston, J. W. 1976. Similarity indices I: what do they measure. BNWL-2152 (Add. 1), Battelle Pacific Northwest Labs., Richland, WA (USA).

Justice, C. O., J. R. G. Townshend, B. N. Holben, and C. J. Tucker. 1985. Analysis of the phenology of global vegetation using meteorological satellite data. International Journal of Remote Sensing 6: 1271-1318.

Karl, T. R., P. D. Jones, R. W. Knight, et al. 1993. A New Perspective on Recent Global Warming: Asymmetric Trends of Daily Maximum and Minimum Temperature. Bulletin of the American Meteorological Society 74, no. 6: 1007-1023.

Kaufman, L., and P. J. Rousseeuw. 1990. Finding groups in data. Wiley New York.

Kerr, M. Kathleen, and Gary A. Churchill. 2001. Bootstrapping cluster analysis: Assessing the reliability of conclusions from microarray experiments. Proceedings of the National Academy of Sciences 98, no. 16 (July 31): 8961-8965. doi:10.1073/pnas.161273698.

Knowles, K., E Njoku, R. Armstrong, and M. Brodzik. 1999. Nimbus-7 SMMR Pathfinder daily EASE-Grid brightness temperatures. Boulder, CO: National Snow and Ice Data Center. Digital media and CD-ROM.

Kudo, G. 1991. Effects of snow-free period on the phenology of alpine plants inhabiting snow patches. Arctic and Alpine Research 23: 436-443.

Laternser, M., and M. Schneebeli. 2003. Long-term snow climate trends of the Swiss Alps (1931-99). International Journal of Climatology 23: 733-750.

Lloyd, D. 1990. A phenological classification of terrestrial vegetation cover using shortwave vegetation index imagery. International Journal of Remote Sensing 11, no. 12: 2269-2279.

MacKay, M. D., F. Seglenieks, D. Verseghy, et al. 2003. Modeling Mackenzie Basin Surface Water Balance during CAGES with the Canadian Regional Climate Model. Journal of Hydrometeorology 4, no. 4 (August 1): 748-767 .

Malingreau, J. P. 1986. Global vegetation dynamics: satellite observations over Asia. International Journal of Remote Sensing 7, no. 9: 1121-1146.

Mccarty, John P. 2001. Ecological Consequences of Recent Climate Change. Conservation Biology 15, no. 2.

McKenna, J. E. 2001. Biological structure and dynamics of littoral fish assemblages in the Eastern Finger Lakes. Aquatic Ecosystem Health & Management 4, no. 1: 91-114.

Mckenna, J.E. 2003. An enhanced cluster analysis program with bootstrap significance testing for ecological community analysis. Environmental Modelling and Software 18, no. 3: 205-220.

Meir, P., P. Cox, and J. Grace. 2006. The influence of terrestrial ecosystems on climate. Trends in Ecology & Evolution 21, no. 5: 254-260.

Milligan, G. W., and M. C. Cooper. 1985. An examination of procedures for determining the number of clusters in a data set. Psychometrika 50, no. 2: 159-179.

Moody, A., and D. M. Johnson. 2001. Land-surface phenologies from AVHRR using the discrete Fourier transform. Remote Sensing of Environment 75: 305-323.

Moulin, S., L. Kergoat, N. Viovy, and G. Dedieu. 1997. Global-Scale Assessment of Vegetation Phenology Using NOAA/AVHRR Satellite Measurements. Journal of Climate 10: 1154-1170.

Nemec, A. F. L., and R. O. Brinkhurst. 1988. Using the bootstrap to assess statistical significance in the cluster analysis of species abundance data. Canadian Journal of Fisheries and Aquatic Sciences 45, no. 6: 965-970.

Pietroniro, A., and R. Leconte. 2005. A review of Canadian remote sensing and hydrology, 1999-2003. Hydrological Processes 19: 285-301.

Pillar, V. D. P. 1999. How sharp are classifications? Ecology 80, no. 8: 2508-2516.

Poff, N. 1996. A hydrogeography of unregulated streams in the United States and an examination of scale-dependence in some hydrological descriptors. Freshwater Biology 36, no. 1: 71-79.

Pulliainen, J., and M. Halliskainen. 2001. Retrieval of regional snow water equivalent from space-borne passive microwave observations. Remote Sensing of Environment 75:76-85.

Rao, A.R., and V. V. Srinivas. 2006. Regionalization of watersheds by hybrid-cluster analysis. Journal of Hydrology 318, no. 1-4: 37-56.

Reed, B. C., J. F. Brown, D. VanderZee, et al. 1994. Measuring phenological variability

from satellite imagery. Journal of Vegetation Science 5, no. 5: 703-714.

Rowe, J. S., and J. W. Sheard. 1981. Ecological land classification: A survey approach. Environmental Management 5: 451-464.

Serreze, M., J. Walsh, F. Chapin, T. Osterkamp, M. Dyurgerov, V. Romanosky, W. Oechel, J. Morison, T. Zhang, and R. Barry. 2000. Observational evidence of recent change in the northern high-latitude environment. Climatic Change 46:159–207.

Sims, R. A., I. G. W. Corns, and K. Klinka. 1996. Global to local: Ecological Land Classification. Environmental Monitoring and Assessment 39, no. 1: 1-10.

Smith, S. P., and R. Dubes. 1980. Stability of a hierarchical clustering. Pattern Recognition 12, no. 3: 177-187.

Sneath, P. H. A., and R. R. Sokal. 1973. Numerical Taxonomy: The Principles and Practice of Numerical Classification. San Francisco.

Sokol, J., T. J. Pultz, and A. E. Walker. 2003. Passive and active airborne microwave remote sensing of snow cover. International Journal of Remote Sensing 24, no. 24: 5327-5344.

Tait, A. 1996. Estimation of snow water equivalent using passive microwave radiation data. Geoscience and Remote Sensing Symposium, 2000. Proceedings. IGARSS 2000. IEEE 2000 International 4:2005-2007.

Unal, Y., T. Kindap, and M. Karaca. 2003. Redefining the climate zones of Turkey using cluster analysis. International Journal of Climatology 23, no. 9: 1045-1055.

Walker, A. E., and A. Silis. 2002. Snow-cover variations over the Mackenzie River basin, Canada, derived from SSM/I passive-microwave satellite data. Annals of Glaciology 34, no. 1: 8-14.

Walker, A., and B. Goodison. 2000. Challenges in determining snow water equivalent over Canada using microwave radiometry. Geoscience and Remote Sensing Symposium, 2000. Proceedings. IGARSS 2000. IEEE 2000 International 4: 1551-1554.

Walker, D. A., J. C. Halfpenny, M. D. Walker, and C. A. Wessman. 1993. Long-Term Studies of Snow-Vegetation Interactions. BioScience 43, no. 5: 287-301.

Walker, M. D., D. A. Walker, J. M. Welker, et al. 1999. Long-term experimental manipulation of winter snow regime and summer temperature in arctic and alpine tundra. Hydrological Processes 13: 2315-2330.

Walther, G. R., E. Post, P. Convey, et al. 2002. Ecological responses to recent climate change. Nature 416: 389-395.

Wiken, E. B. 1986. Terrestrial ecozones of Canada. Ecological Land Classification. Environment Canada.

Wiken, E., D. Gauthier, I. Marshall, K. Lawton, and H. Hirvonen. 1996. A Perspective on Canada's Ecosystems, Occasional Paper No. 14, Canadian Council on Ecological Areas, Ottawa, ON, Canada.

Wulder, M., T. Nelson, C. Derksen, and D. Seemann. 2007. Snow cover variability across central Canada (1978-2002) derived from satellite passive microwave data. Climatic Change 82: 113-130.

Chapter 4.0 References

Barnett, T. P., L. Dümenil, U. Schlese, E. Roeckner, and M. Latif. 1989. The Effect of Eurasian Snow Cover on Regional and Global Climate Variations. Journal of the Atmospheric Sciences 46: 661-686.

Bojariu, R., and L. Gimeno. 2003. The role of snow cover fluctuations in multiannual NAO persistence. Geophyiscal Research Letters 30: 1156.

Brown, R. 2000. Northern Hemisphere snow cover variability and change, 1915-1997. Journal of Climate 13: 2339-2355.

Cohen, J., and D. Rind. 1991. The Effect of Snow Cover on the Climate. Journal of Climate 4: 689-706.

Derksen, C., E. LeDrew, and B. Goodison. 1998a. Application of the Getis statistic to hemispheric and regional scale passive microwave derived snow water equivalent imagery. Geoscience and Remote Sensing Symposium Proceedings, IGARSS '98. 1998 IEEE International 2: 977-979.

Derksen, C., W. Wulder, E. LeDrew, and B. Goodison. 1998b. Associations between spatially autocorrelated patterns of SSM/I derived Prairie snow cover and atmospheric circulation. Hydrological Processes 12: 2307-2316.

Egenhofer, K.J., and R.G. Golledge. 1997. Spatial and temporal reasoning in Geographic Information Sytems. New York: Oxford University Press.

Langran, G. 1990. Tracing temporal information in an automated nautical charting system. Cartography and Geographic Information Systems 17: 291-299.

Langran, G. 1992. Time in Geographic Information Systems. New York: Taylor & Francis.

Laternser, M., and M. Schneebeli. 2003. Long-term snow climate trends of the Swiss Alps (1931-99). International Journal of Climatology 23: 733-750.

Maxwell, B. 1992. Arctic climate: potential for change under global warming. Arctic Ecosystems in a Changing Climate: An Ecophysiological Perspective: 11–34.

——— 1997. Recent climate patterns in the Arctic. Global Change and Arctic Terrestrial Ecosystems: 21-46.

Peuquet, D.J. 2002. Representations of space and time. New York: Guilford.

QGIS Development Core Team (2008). Quantum GIS. GNU General Public License, URL: http://www.qgis.org/

R Development Core Team (2007). R: A language and environment for statistical computing. R Foundation for Statistical Computing, Vienna, Austria. ISBN 3-900051-07-0, URL: http://www.R-project.org

Rey, S., and M. Janikas. 2006. STARS: Space-time analysis of regional systems. Geographical Analysis 38: 67-86.